

Flanders
State of
the Art

21_104_5
FH reports

Modelling Belgian Coast: ScaldisCoast

Sub report 5 – Release notes ScaldisCoast 2026

DEPARTMENT
MOBILITY &
PUBLIC
WORKS

www.flandershydraulics.be

Modelling Belgian Coast: ScaldisCoast

Sub report 5 – Release notes ScaldisCoast 2026

Wang, L.; Kolokythas, G.; Breugem, W.A.; De Maerschalck, B.

Flanders Hydraulics
Flanders State of the Art

Cover figure © The Government of Flanders, Department of Mobility and Public Works, Flanders Hydraulics

Legal notice

Flanders Hydraulics is of the opinion that the information and positions in this report are substantiated by the available data and knowledge at the time of writing.
The positions taken in this report are those of Flanders Hydraulics and do not reflect necessarily the opinion of the Government of Flanders or any of its institutions.
Flanders Hydraulics nor any person or company acting on behalf of Flanders Hydraulics is responsible for any loss or damage arising from the use of the information in this report.

Copyright and citation

© The Government of Flanders, Department of Mobility and Public Works, Flanders Hydraulics 2026
D/2026/3241/231

This publication should be cited as follows:

Wang, L.; Kolokythas, G.; Breugem, W.A.; De Maerschalck, B. (2026). Modelling Belgian Coast: ScaldisCoast: Sub report 5 – Release notes ScaldisCoast 2026. Version 4.0. FH Reports, 21_104_5. Flanders Hydraulics: Antwerp

Reproduction of and reference to this publication is authorised provided the source is acknowledged correctly.

Document identification

Customer:	Flanders Hydraulics	Ref.:	WL2026R21_104_5
Keywords (3-5):	Coastal modelling, sediment transport		
Knowledge domains:	Hydraulics and sediment > Hydrodynamics > Waves > Numerical modelling Hydraulics and sediment > Hydrodynamics > Tides > Numerical modelling Hydraulics and sediment > Sediment > Sediment transport > Numerical modelling		
Text (p.):	34	Appendices (p.):	6
Confidential:	☒ No	☒ Available online	

Author(s):	Wang, L.; Kolokythas, G.; Breugem, W.A.; De Maerschalck, B.

Control

	Name	Signature
Reviser(s):	Breugem, A.	Getekend door:Breugem Willem Alexand Getekend op:2026-08-14 16:46:38 +02:0 Reden:I approve this document Breugem Alexander
Project leader:	De Maerschalck, B.	Getekend door:De Maerschalck Bart Getekend op:2026-08-14 15:43:45 +02:0 Reden:Ik keur dit document goed De Maerschalck Bart Vlaamse overheid

Approval

Head of Division:	Bellafkih, K.	Getekend door:Bellafkih Abdelkarim Getekend op:2026-08-14 21:01:30 +02:0 Reden:Ik keur dit document goed Bellafkih Abdelkarim Vlaamse overheid

Abstract

This report presents the release notes for the ScaldisCoast 2026 model, focusing on improvements in sediment transport modelling for the Belgian coast. In previous applications, the widely used Bijker formulation was found to exhibit strong sensitivity to grain size, leading to unrealistic variability in predicted transport rates. In addition, the formulation is primarily driven by wave action, resulting in limited sediment transport in areas with weak or absent wave influence, such as estuaries.

Furthermore, the sediment distribution was represented using only two grain-size fractions, with their relative proportions derived from transport rates associated with the Bijker formulation. As a result, the sediment composition became dependent on the selected transport formulation, limiting the generality and transferability of the modelling approach.

To address these limitations, alternative sediment transport formulations are investigated, with a particular focus on the formulation of Wu & Lin. A schematised numerical model is first applied to systematically evaluate the sensitivity of different formulations to grain size and hydrodynamic forcing. **A multi-fraction sediment approach is introduced** to provide a more realistic and formulation-independent representation of sediment composition. In addition, an advection-diffusion transport approach is implemented to enable the representation of **cross-shore sediment transport within the 2D modelling framework**.

The updated modelling framework is subsequently validated using the full ScaldisCoast model through a series of real-case applications along the Belgian coast, covering both long-term and short-term morphodynamic processes. These include bed evolution near the western dam of Zeebrugge, erosion at Wenduine, annual sedimentation at Blankenberge, and storm-induced siltation during Storm Ciara (2020).

The results demonstrate that all tested formulations reproduce the overall magnitude of sediment transport; however, differences remain in the spatial distribution of sedimentation and erosion. The study highlights the successful application of the Wu & Lin formulation with multiple sediment fractions and provides a more robust and transferable framework for coastal morphodynamic modelling.

Contents

Abstract III
Contents V
List of tables VI
List of figures VII
1 Introduction 1
1.1 Background 1
1.2 Objectives 1
1.3 Scope 2
1.4 Structure of the Report 2
2 Schematised model 3
2.1 Model domain and bathymetry 3
2.2 Model boundaries 4
2.3 Model results 5
2.3.1 Comparison among different transport formulae 5
2.3.2 Application of multiple fractions 8
2.3.3 Advection-diffusion transport using the formula Wu & Lin 11
3 Morphology model validation with the transport formula of Wu & Lin 13
3.1 Bed evolution next to the western dam of Zeebrugge 13
3.2 Erosion in front of Wenduine 17
3.3 Annual sedimentation at Blankenberge 23
3.4 Storm-induced siltation at Blankenberge 27
4 Conclusions 33
References 34
Appendix A Coupled model settings for TELEMAC version v8p4 ..... A1
A.1 Settings of TELEMAC-2D module A1
A.2 Settings of TOMAWAC module A3
A.3 Settings of GAIA module A4

List of tables

Table 1: Overview of the four model configurations evaluated in this study. 13

Table 2: Comparison between measured and modelled net volume change within different polygons for the validation case: bed evolution next to the Western dam of Zeebrugge. 17

Table 3: Comparison between measured and modelled net erosion in front of Wenduine. 22

Table 4: Overview of the model settings used for the validation of annual sedimentation at Blankenberge. 23

Table 5: Comparison between measured and modelled annual sedimentation at Blankenberge. 27

Table 6: Overview of the model settings used for the validation of storm-induced siltation at Blankenberge. 27

Table 7: Comparison between measured and modelled net and gross volume changes within separated zones for the validation case: storm-induced siltation at Blankenberge. 31

List of figures

Figure 1: Computational mesh of the schematised model. 3

Figure 2: Bathymetry of the schematised model. 4

Figure 3: Boundaries of hydrodynamics simulation (pink circle: zero flow; green triangle: 10-m water depth; black square: closed boundaries). 4

Figure 4: Boundaries of wave simulation (green triangle: open boundaries; black square: closed boundaries). 5

Figure 5: Comparison of sediment transport rates predicted by five transport formulations: Wu & Lin, SVR, VR07, VR93, and Bijker for varying median grain sizes (D_{50}) under significant wave heights of 1 m, 2 m, and 3 m. Note that the y-range is different for the three graphs. 6

Figure 6: Sediment transport rates predicted by the transport formulation of Bijker. Note that the y-range is different for the three graphs. 7

Figure 7: Grain size distribution determined by different ratios D_{90}/D_{50} for D_{50} = 200 µm. 8

Figure 8: Grain size distribution represented by ten fractions ranging from 100 µm to 1000 µm for a sediment mixture with D_{90}/D_{50} = 1.5 and D_{50} = 200 µm. 9

Figure 9: Sediment transport rates predicted by the transport formulation of Wu & Lin for uniform and nonuniform (multi-fraction) sediment beds. Note that the y-range is different for the three graphs..... 10

Figure 10: Sediment transport rates predicted by the transport formulation of Wu & Lin using bedload and advection-diffusion equations. 12

Figure 11: Measured ten-year bed evolution between 1999 and 2009, in the area next to the western dam of Zeebrugge (reproduced from Verwaest et al., 2011). 14

Figure 12: Modelled ten-year bed evolution using Bijker formula, bedload equation and two fractions without cross-shore sediment transport, in the area next to the western dam of Zeebrugge (model run HSW113_K17a). 15

Figure 13: Modelled ten-year bed evolution using Wu & Lin formula, bedload equation and ten fractions without cross-shore sediment transport, in the area next to the western dam of Zeebrugge (HSW113_S05b). 15

Figure 14: Modelled ten-year bed evolution using Wu & Lin formula, advection-diffusion equation and ten fractions without cross-shore sediment transport, in the area next to the western dam of Zeebrugge (HSW113_S06c). 16

Figure 15: Modelled ten-year bed evolution using Wu & Lin formula, advection-diffusion equation and ten fractions with cross-shore sediment transport, in the area next to the western dam of Zeebrugge (HSW113_S06a). 16

Figure 16: Measured one-year morphological change at Wenduine. 18

Figure 17: Modelled one-year morphological change at Wenduine, using Bijker formula, bedload equation and two fractions without cross-shore sediment transport. 19

Figure 18: Modelled one-year morphological change at Wenduine, using Wu & Lin formula, bedload equation and ten fractions without cross-shore sediment transport. 20

Figure 19: Modelled one-year morphological change at Wenduine, using Wu & Lin formula, advection-diffusion equation and ten fractions without cross-shore sediment transport. 21

Figure 20: Modelled one-year morphological change at Wenduine, using Wu & Lin formula, advection-diffusion equation and ten fractions with cross-shore sediment transport. 22

Figure 21: Flow (left) and wave (right) meshes in area around Blankenberge. 23

Figure 22: Estimated annual sedimentation in the entrance channel for the port of Blankenberge (reproduced from Teurlincx et al., 2009). 24

Figure 23: Modelled 1-year bed evolution with representative tide and wave/wind over a half year (MorFac =2), in the area around the port of Blankenberge, using Bijker formula, bedload equation and two fractions without cross-shore sediment transport..... 25

Figure 24: Modelled 1-year bed evolution with representative tide and wave/wind over a half year (MorFac =2), in the area around the port of Blankenberge, using Wu & Lin formula, bedload equation and ten fractions without cross-shore sediment transport..... 25

Figure 25: Modelled 1-year bed evolution with representative tide and wave/wind over a half year (MorFac =2), in the area around the port of Blankenberge, using Wu & Lin formula, advection-diffusion equation and ten fractions without cross-shore sediment transport. 26

Figure 26: Modelled 1-year bed evolution with representative tide and wave/wind over a half year (MorFac =2), in the area around the port of Blankenberge, using Wu & Lin formula, advection-diffusion equation and ten fractions with cross-shore sediment transport..... 26

Figure 27: Measured sedimentation in the entrance channel for the port of Blankenberge during the Ciara Storm. 29

Figure 28: Modelled sedimentation in the entrance channel for the port of Blankenberge during the Ciara Storm, using Bijker formula, bedload equation and two fractions without cross-shore sediment transport.29

Figure 29: Modelled sedimentation in the entrance channel for the port of Blankenberge during the Ciara Storm, using Wu & Lin formula, bedload equation and ten fractions without cross-shore sediment transport. 30

Figure 30: Modelled sedimentation in the entrance channel for the port of Blankenberge during the Ciara Storm, using Wu & Lin formula, advection-diffusion equation and ten fractions without cross-shore sediment transport..... 30

Figure 31: Modelled sedimentation in the entrance channel for the port of Blankenberge during the Ciara Storm, using Wu & Lin formula, advection-diffusion equation and ten fractions with cross-shore sediment transport..... 31

Figure 32: Piles located along both sides of the entrance channel at Blankenberge port..... 32

1 Introduction

1.1 Background

In previous applications of the ScaldisCoast model, the Bijker sediment transport formulation was employed as a standard approach. Although this formulation has been widely applied, several limitations have been identified.

First, the predicted sediment transport rates were found to be highly sensitive to the grain size, leading to unrealistic variability in the predicted transport rate. Second, the Bijker formulation is primarily driven by wave-induced processes, resulting in limited sediment transport in areas with weak or absent wave influence, such as estuaries.

In addition, the sediment distribution map used in earlier studies consisted of only two grain-size fractions. The relative proportions of these fractions were determined based on the transport rate associated with the median grain size (D_{50}) using the Bijker formulation (Kolokythas et al., 2021). As a result, the sediment composition becomes dependent on the selected transport formulation. This introduces a lack of general applicability when alternative transport formulations are used, as the sediment distribution would need to be redefined accordingly.

These limitations highlight the need for a more robust and universally applicable modelling framework, in which sediment transport predictions are less sensitive to grain size, applicable across different hydrodynamic environments, and independent of the specific transport formulation.

1.2 Objectives

The main objective of this report is to improve and evaluate the sediment transport modelling approach within the ScaldisCoast model by addressing limitations identified in previous studies. Specifically, the study aims to:

- Reduce the sensitivity of sediment transport predictions to the grain size;
- Improve the prediction of sediment transport in environments with limited wave influence, such as estuaries;
- Develop a formulation-independent approach to represent spatially varying D_{50};
- Evaluate the performance of alternative transport formulations, with particular emphasis on the Wu & Lin formulation;
- Assess the application of an advection-diffusion approach for sediment transport that incorporates wave induced cross-shore sediment transport as developed in Kolokythas *et al.* (2024);
- Validate the updated model against observed morphological changes.

1.3 Scope

The scope of this report includes both schematised model tests and real-case validations using the full ScaldisCoast model. The schematised model is used to efficiently analyse the behaviour of sediment transport formulations under well-controlled conditions. The validated model settings are then applied to four representative cases along the Belgian coast:

- Long-term bed evolution near the western dam of Zeebrugge;
- One-year erosion in front of Wenduine;
- Annual sedimentation in the entrance channel of Blankenberge;
- Short-term storm-induced siltation during Storm Ciara (2020).

The analysis focuses on both qualitative pattern reproduction and quantitative comparison of sediment volumes.

1.4 Structure of the Report

This report is structured as follows:

- Chapter 2 presents the schematised model setup and the sensitivity analysis of different sediment transport formulations;
- Chapter 3 describes the validation of the updated model using real-case applications along the Belgian coast;
- Chapter 4 summarises the main findings and provides conclusions and recommendations for future model development and application.

2 Schematised model

A schematised numerical model was developed to enable rapid assessment of the differing behaviours of multiple sediment-transport formulations with controlled identical hydrodynamic and wave conditions. The simplified model uses a uniform computational mesh and an idealised bathymetry to minimise the influence of complex geometry and boundary conditions, allowing differences in predicted sediment transport to be attributed primarily to the transport formulations themselves. The model is used to

1. compare the behaviour of different sediment transport formulae;
2. assess the influence of representing the seabed as uniform and multi-fraction sediments;
3. evaluate the implementation of the advection-diffusion sediment transport approach.

2.1 Model domain and bathymetry

In this study, the schematised model was developed based on the littoral test case included in the GAIA module of TELEMAC (Open Telemac-Mascaret, 2019). The model domain extends 1000 m in the longitudinal direction (X-axis) and 200 m in the transverse direction (Y-axis). The model mesh consists of a uniform set of quadrilateral elements with a width of 5 m and a length of 20 m (Figure 1). The bathymetry varies linearly from -10 m at the lower boundary (y =0 m) to -0.1 m at the upper boundary (y =200 m), forming a constant bed slope in the transverse direction (Figure 2).

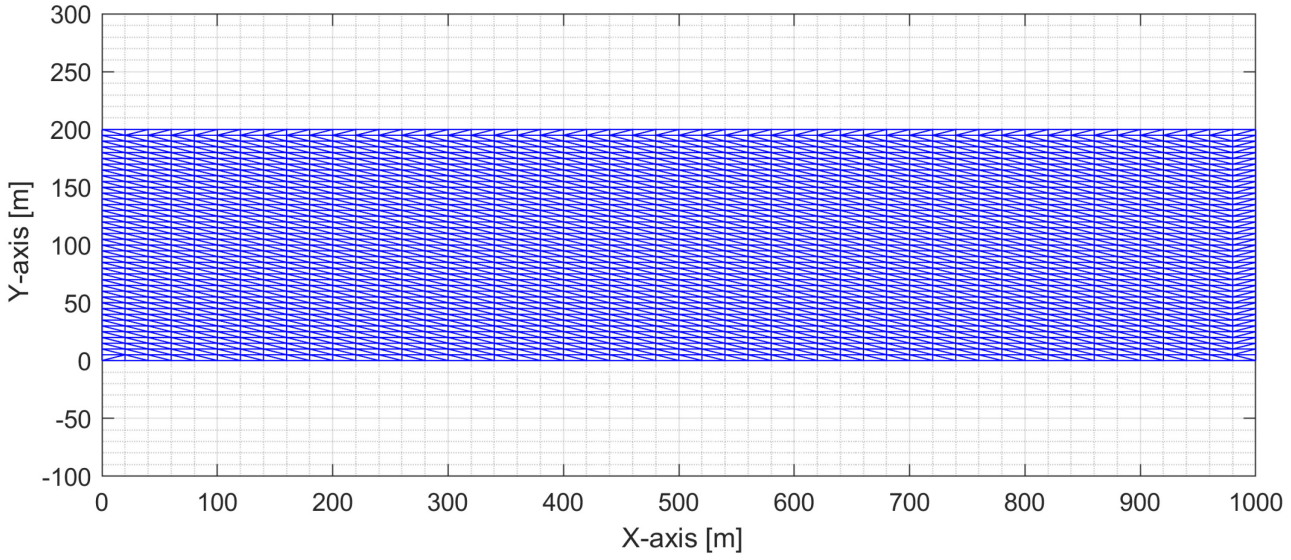


Figure 1: Computational mesh of the schematised model.

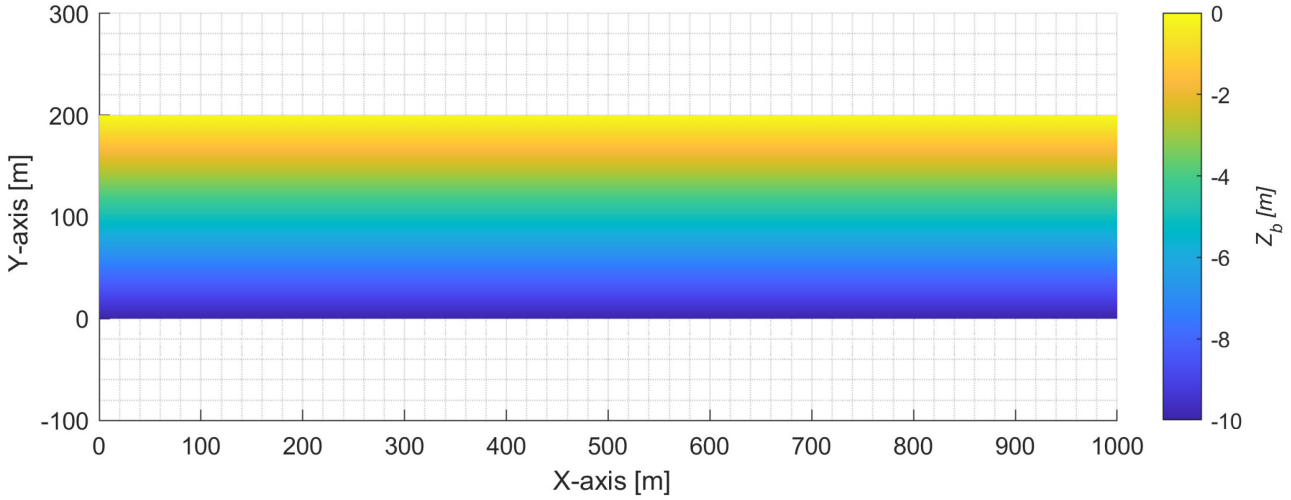


Figure 2: Bathymetry of the schematised model.

2.2 Model boundaries

Figure 3 and Figure 4 present the boundary configurations of the hydrodynamic and wave models, respectively. For the hydrodynamic simulation, a constant water depth of 10 m is prescribed at the offshore boundary of the computational domain . The two lateral boundaries are specified as zero-flow boundaries, and the upper boundary is treated as a closed boundary.

For the wave simulation, a constant wave condition is imposed along all open boundaries, including the offshore boundary and the two lateral boundaries. The imposed wave forcing is defined by the significant wave height, peak wave period, and mean wave direction.

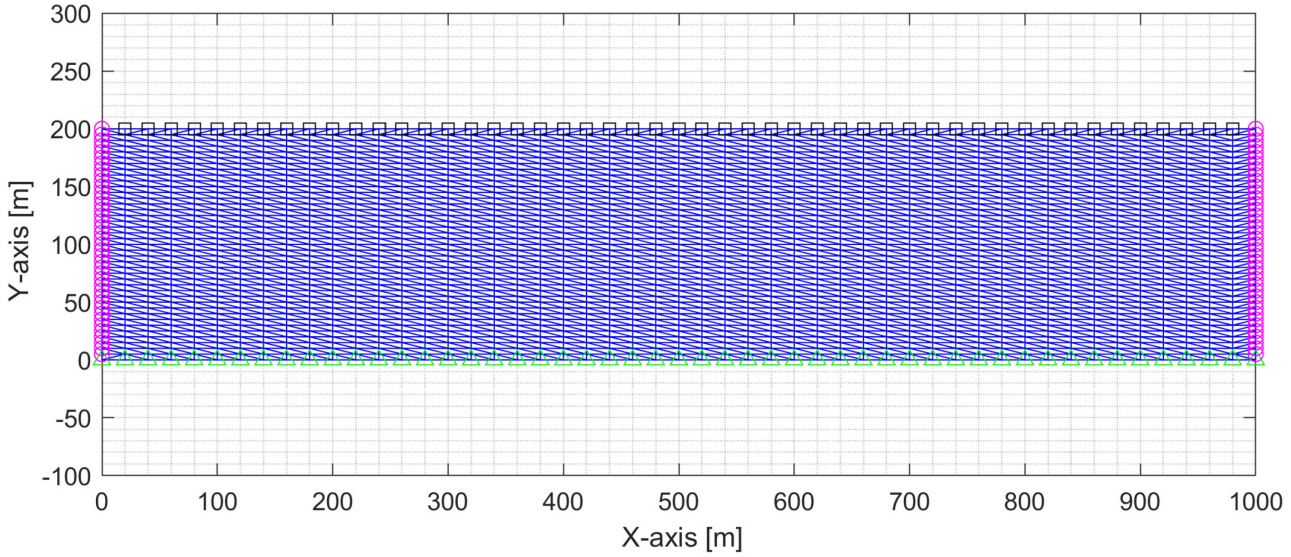


Figure 3: Boundaries of hydrodynamics simulation
(pink circle: zero flow; green triangle: 10-m water depth; black square: closed boundaries).

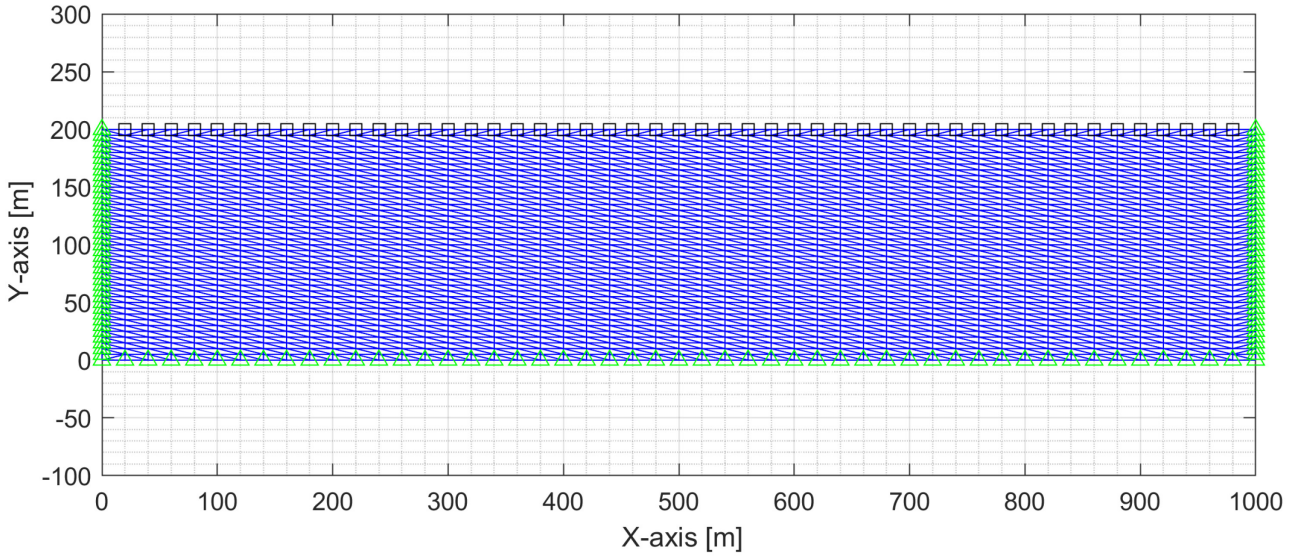


Figure 4: Boundaries of wave simulation (green triangle: open boundaries; black square: closed boundaries).

2.3 Model results

2.3.1 Comparison among different transport formulae

Figure 5 presents the sediment transport rates predicted by five formulations: Wu & Lin (*Wu & Lin, 2014*), SVR (*Soulsby, 1997*), VR07 (*van Rijn, 2007*), VR93 (*van Rijn, 1993*), and Bijker (*Bijker, 1971*), which vary with median grain size (D_{50}) under different significant wave heights of 1 m, 2 m, and 3 m. For the VR93 formulation, suspended sediment transport is computed using an advection-diffusion approach. The results show the dependence of transport magnitude on both grain size and wave forcing. The substantial variability in predicted rates is exhibited among the different formulations.

It can be observed that all formulations predict increasing transport rates with increasing wave height. Bijker and Wu & Lin generally predict the highest transport rates, particularly for fine sediments ($\leqslant$ 200 µm), whereas the SVR and VR07 formulations produce comparatively low transport rates with less variation across the tested grain sizes. The VR93 formulation gives intermediate transport rates, with a moderate decline as grain size increases.

A notable feature is the strong sensitivity of the Bijker formulation to grain size. For D_{50} = 100 µm, the transport rates predicted by Bijker exceed the plotting range of the figures, indicating exceptionally large transport estimates. As a result, a separate figure is provided to display the Bijker predictions in full range (Figure 6).

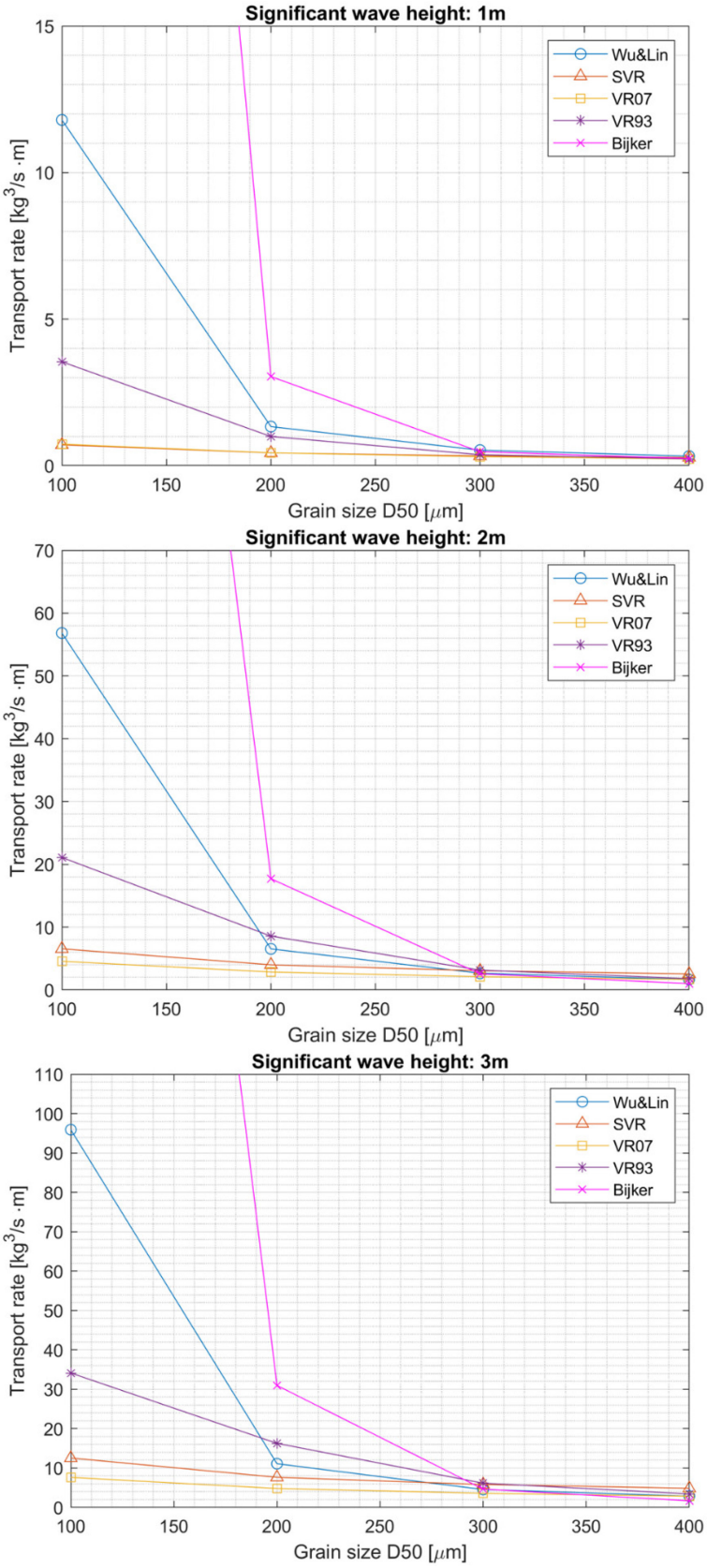


Figure 5: Comparison of sediment transport rates predicted by five transport formulations: Wu & Lin, SVR, VR07, VR93, and Bijker for varying median grain sizes (D_{50}) under significant wave heights of 1 m, 2 m, and 3 m.
Note that the y-range is different for the three graphs.

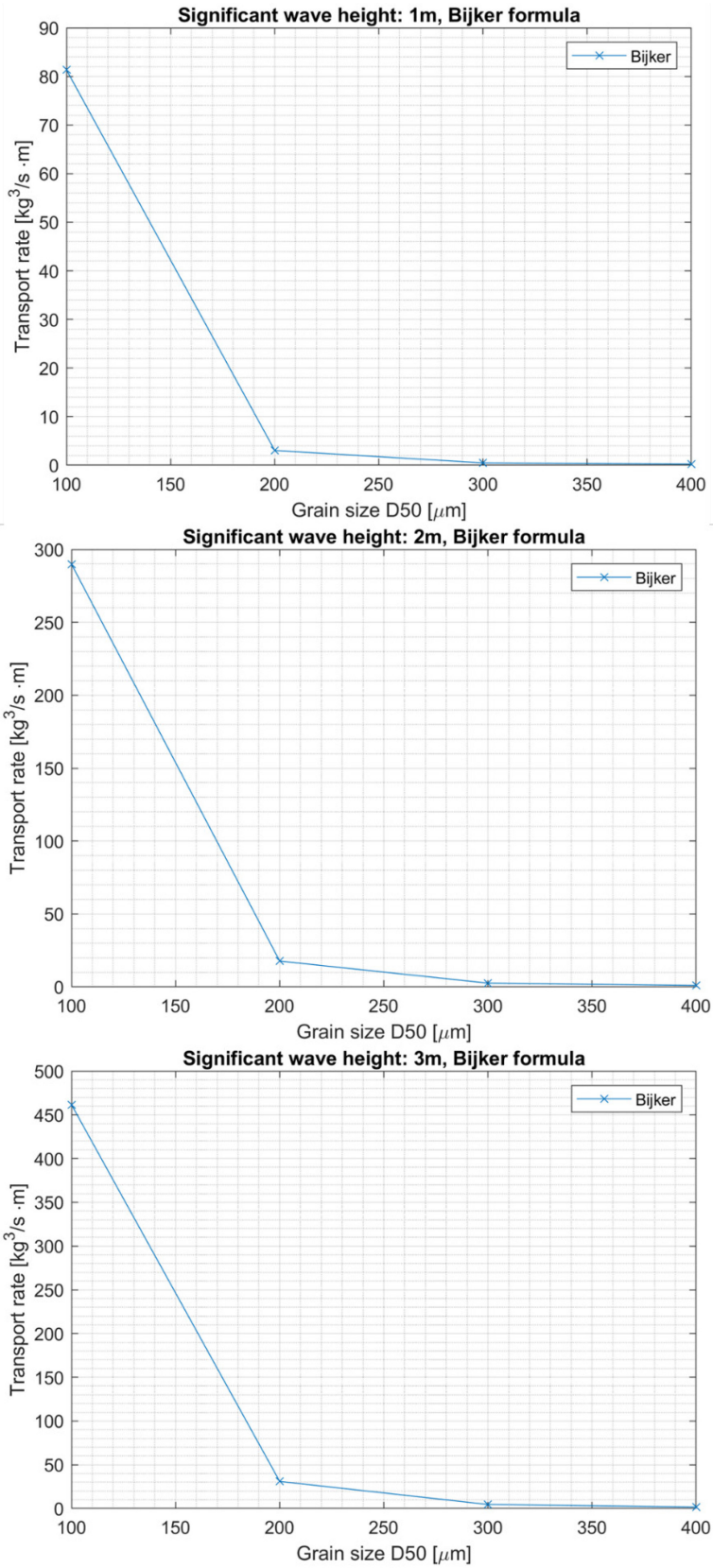


Figure 6: Sediment transport rates predicted by the transport formulation of Bijker.
Note that the y-range is different for the three graphs. .

2.3.2 Application of multiple fractions

In natural coastal environments, sediments are typically nonuniform or graded rather than uniform. The transport behaviour of nonuniform sediments can differ from that of uniform sediments, even when both have the same median grain size D_{50}. In the formulation of Wu & Lin, the hiding and exposure effects on different grain-size fractions are considered, enabling the model to represent the reduced mobility of finer particles due to hiding effect and the enhanced mobility of coarser particles due to exposure effect within a mixed sediment bed.

In addition to the median grain size D_{50}, D_{90} is also an important parameter in some transport formulations. The value of this parameter represents the grain size at which 90% of the material is finer and 10% is coarser. For a nonuniform bed composed of multiple sediment fractions, the ratio D_{90}/D_{50} provides an indication of the grading of the sediment mixture and helps determine the overall shape of the grain size distribution (Figure 7). In this study, a value of 1.5 is used for D_{90}/D_{50} following Soulsby (1997), and ten fractions ranging from 100 µm to 1000 µm are employed to approximate the grain size distribution (Figure 8). The grain size distribution is parametrized using a lognormal distribution.

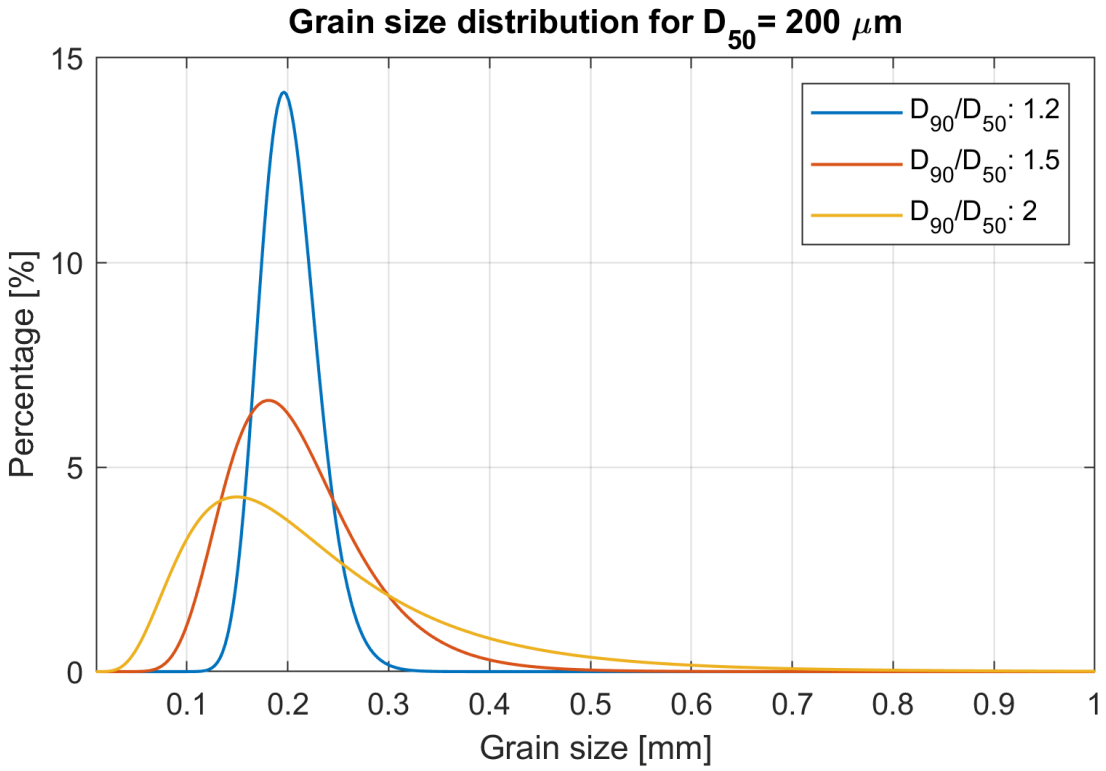


Figure 7: Grain size distribution determined by different ratios D_{90}/D_{50} for D_{50} = 200 µm.

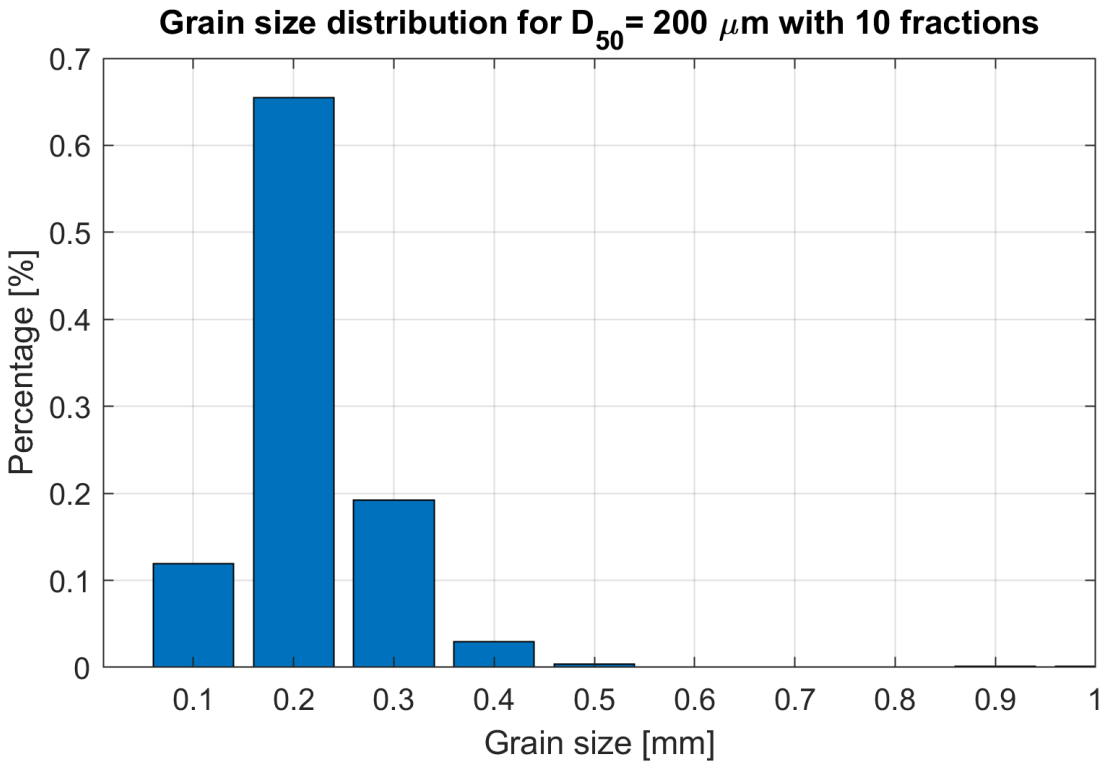


Figure 8: Grain size distribution represented by ten fractions ranging from 100 µm to 1000 µm for a sediment mixture with D_{90}/D_{50} = 1.5 and D_{50} = 200 µm.

Figure 9 compares the sediment transport rates predicted by the formulation of Wu & Lin between uniform and nonuniform (multi-fraction) sediment beds. For all wave conditions, transport rates decrease with increasing grain size, and larger wave heights lead to higher predicted transport rates.

Although the transport rates predicted for the uniform and multi-fraction sediment beds are generally very similar across the full grain-size range, the results still demonstrate that hiding and exposure effects explicitly influence the sediment transport. For the finest grain size (100 µm), the multi-fraction prediction yields slightly lower transport rates due to the hiding effect on the fine particles within the graded sediment mixture. Conversely, for the coarser grain sizes (200 and 250 µm), the multi-fraction approach produces slightly higher transport rates as a result of exposure effects on the coarser particles. As grain size becomes larger, the two predictions gradually converge, indicating that the interaction among different grain sizes becomes negligible.

This multi-fraction approach is independent of the selected transport formulation to represent the sediment distribution map, thereby overcoming the limitations of previous approaches in which sediment composition was directly linked to the transport formulation.

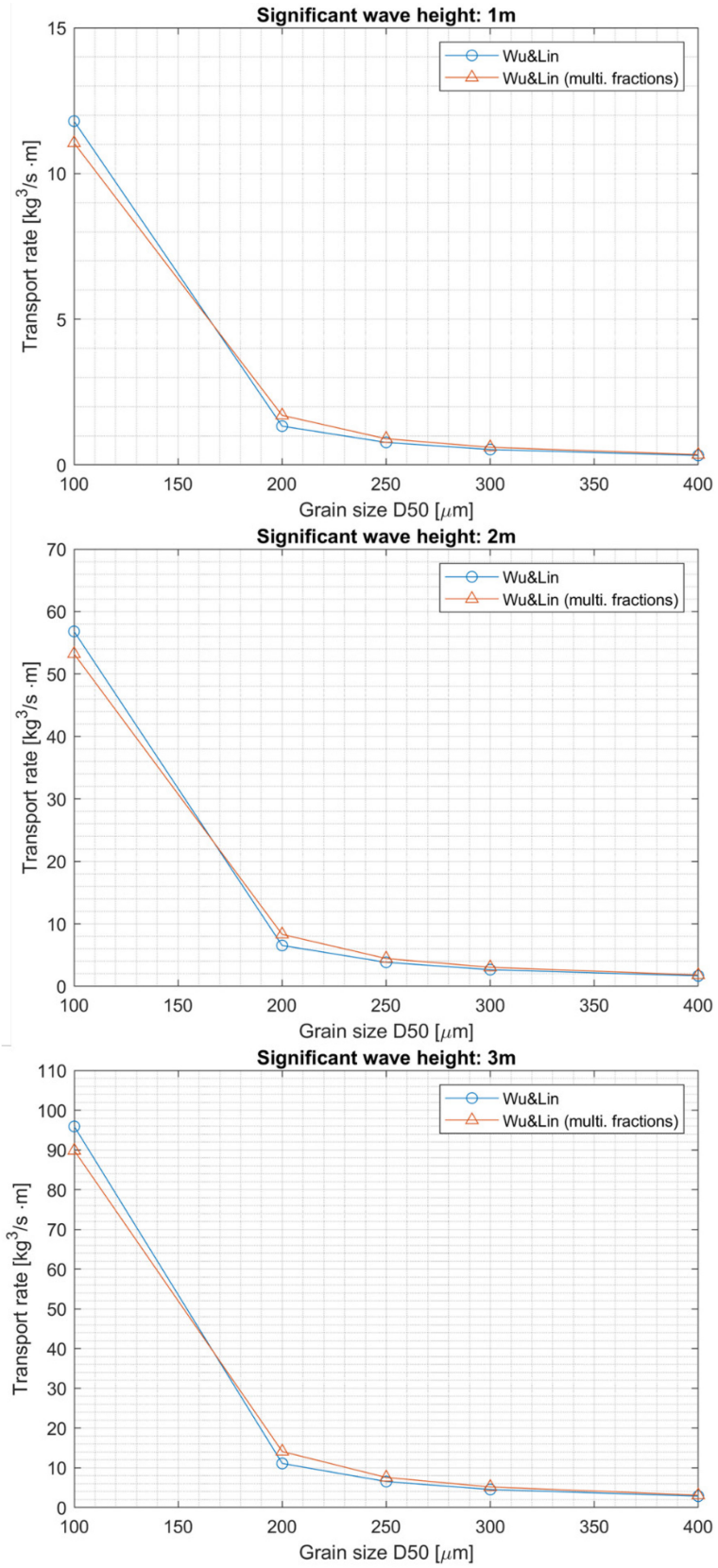


Figure 9: Sediment transport rates predicted by the transport formulation of Wu & Lin for uniform and nonuniform (multi-fraction) sediment beds. Note that the y-range is different for the three graphs.

2.3.3 Advection-diffusion transport using the formula Wu & Lin

In the advection-diffusion approach (strongly inspired by the approach taken in XBeach), an advection diffusion equation is used to determine the depth averaged sediment concentration (Fonias et al. 2021; Kolokythas et al. 2024). Erosion and deposition are taken into account through source terms. The erosion is determined from the equilibrium sediment concentration, which is determined from the total load equation. Hence, in this approach the total load is taken into account, not just the suspended load, as is commonly done in TELEMAC. The advection diffusion approach , had the advantage over the classical approach (which uses the total load equation in combination with the Exner equation), that some additional smoothing is added in a physically consistent way. Further, cross-shore sediment transport can easily be taken into account in this approach.

Figure 10 compares sediment transport rates computed using the bedload and advection–diffusion equations for the multi-fraction case. The two lines almost coincide, which indicates a very similar model behaviour for both approaches. This agreement demonstrates consistency in the computed sediment transport when switching from the bedload equation to the advection-diffusion equation.

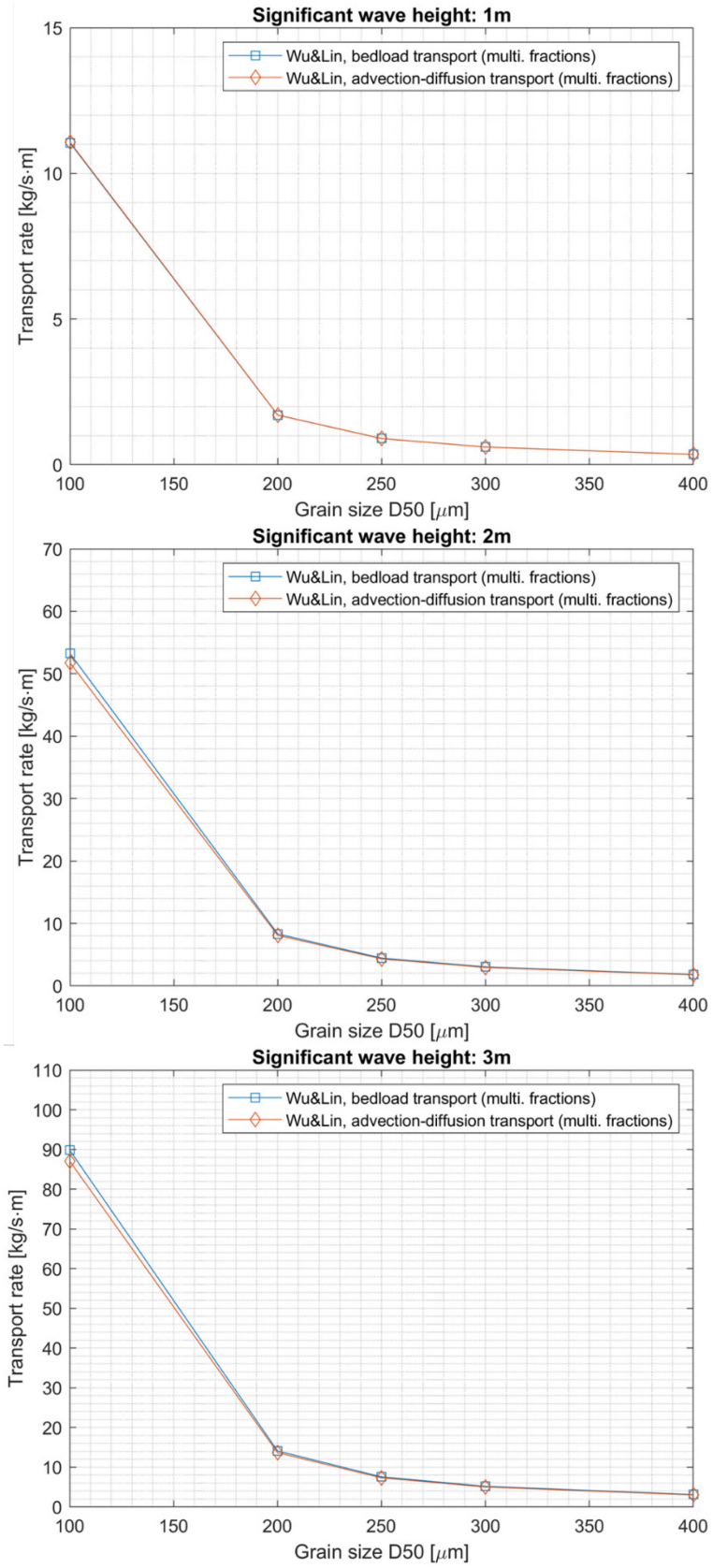


Figure 10: Sediment transport rates predicted by the transport formulation of Wu & Lin using bedload and advection-diffusion equations.

3 Morphology model validation with the transport formula of Wu & Lin

Following sensitivity runs with different settings using the schematised model (chapter 2), the Scaldis-Coast model, which covers the entire Belgian coast (Kolokythas et al., 2021), is applied to validate the new settings under real-case conditions. A detailed description of the new model settings is provided in Appendix A.1–A.3. The morphological validation is performed for four cases, which are presented in the separate sections below.

The four different settings used for the morphological validation of the Scaldis-Coast model are summarized in the table below:

Table 1: Overview of the four model configurations evaluated in this study.

Series	Transport formulation	Sediment fractions	Transport approach	Cross-shore transport	Remarks
A	Bijker (1971)	2 fractions (200, 500 µm)	Total-load	No	Default settings in the previous study (Wang et al. 2026)
B	Wu & Lin (2014)	10 fractions (100 - 1000 µm, 100 µm interval)	Total-load	No	Multi-fraction implementation
C	Wu & Lin (2014)	10 fractions (100 - 1000 µm, 100 µm interval)	Advection–diffusion	No	Using the advection–diffusion transport approach
D	Wu & Lin (2014)	10 fractions (100 - 1000 µm, 100 µm interval)	Advection–diffusion	Yes	Inclusion of cross-shore sediment transport

3.1 Bed evolution next to the western dam of Zeebrugge

In the study of Verwaest et al. (2011), the area near the western dam of Zeebrugge is divided into three zones: green, red and pink polygons (Figure 11). The erosion (in blue) and sedimentation (in brown) volumes are quantified in this study area. The total littoral drift is estimated based on the measured volumetric trends with an assumption that no sediment is brought into the longshore zone from offshore areas.

The objective of the present case study is to validate the modelled long-term longshore sediment transport rate induced by waves and currents. The modelled sedimentation/erosion maps obtained using four different settings are presented in Figure 12 - Figure 15 (dark blue: strong erosion; dark red: strong sedimentation).

All four settings successfully reproduce the pronounced sedimentation observed within the green polygon, although the magnitude is underestimated to varying extents. Setting C yields the best agreement, with an underestimation of 30%, whereas Setting D shows the largest underestimation, reaching 54% (Table 2). It should be noted, however, that Setting D predicts stronger sedimentation near the upper part of the dam. As this area falls outside the green polygon, the additional sedimentation is not included for the volume calculation.

In the red polygon, all settings predict net sedimentation; however, the location of the modelled sedimentation maxima is shifted more nearshore compared to the observation. For the net sedimentation volume, Setting B performs best, with an overestimation of 63%, while Setting D again shows the largest discrepancy, overestimating sedimentation by 123% (Table 2). In comparison, Setting C without cross-shore sediment transport (CST) overestimates the sedimentation by 80%. The larger overestimation in Setting D suggests that the inclusion of CST enhances the sedimentation within the red polygon. This increase appears to result from the stronger erosion predicted in the pink polygon, which supplies more sediment to the adjacent red polygon.

Within the pink polygon, the general erosion pattern is captured by all four settings. Nevertheless, Settings A and B predict net sedimentation, which contradicts the net erosion reported by Verwaest et al. (2011). In contrast, Settings C and D correctly reproduce net erosion. Setting D, however, substantially overestimates the erosion magnitude by a factor 6 (Table 2), indicating that the inclusion of CST leads to excessive erosion in this area. This excessive erosion is consistent with the increased sedimentation predicted within the neighbouring red polygon.

Overall, the results obtained with Settings A, B, and C are very similar. By contrast, the inclusion of cross-shore transport in Setting D results in substantially reduced sedimentation in the green polygon and significantly enhanced erosion in the pink polygon.

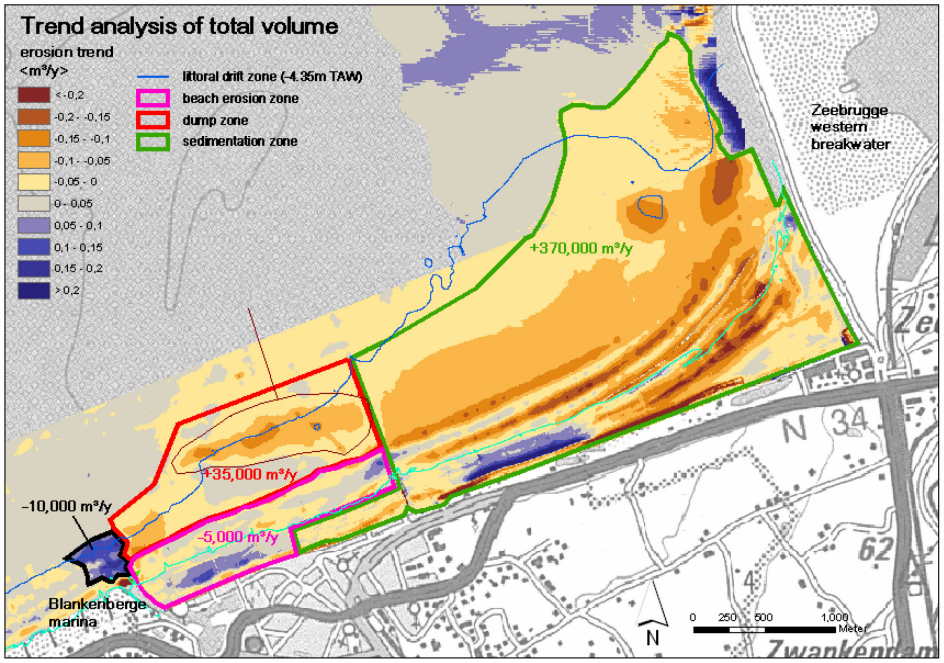


Figure 11: Measured ten-year bed evolution between 1999 and 2009, in the area next to the western dam of Zeebrugge (reproduced from Verwaest et al., 2011).

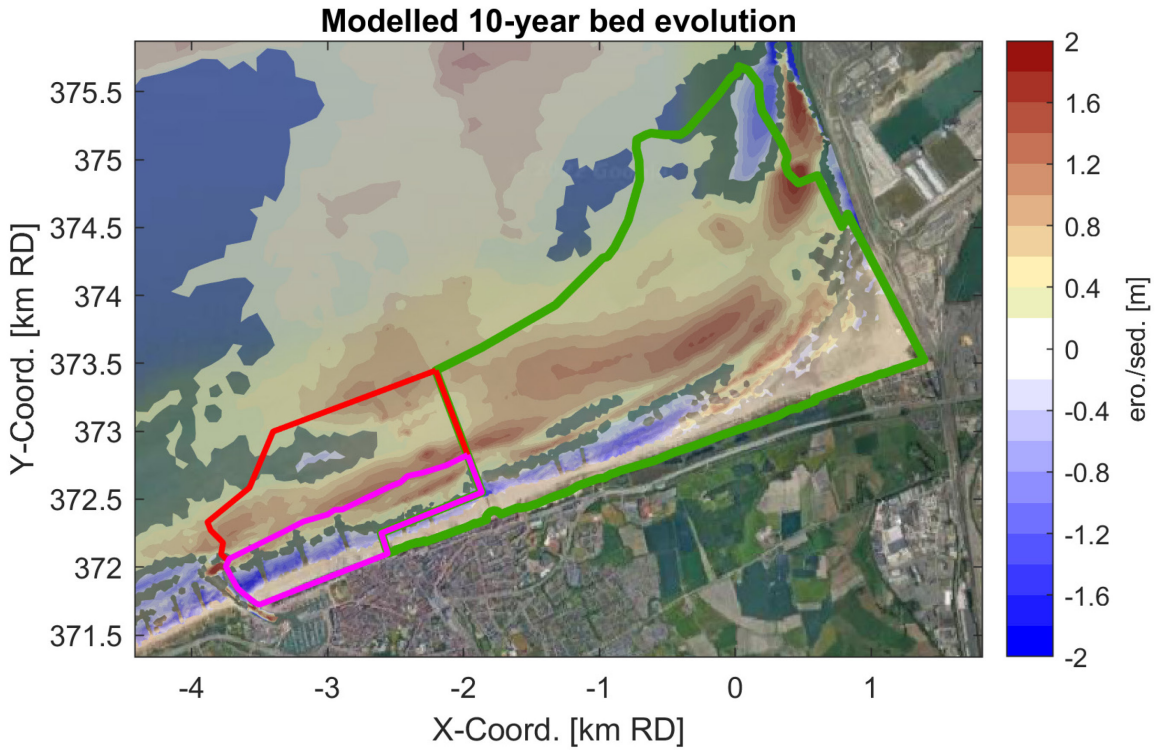


Figure 12: Modelled ten-year bed evolution using Bijker formula, bedload equation and two fractions without cross-shore sediment transport, in the area next to the western dam of Zeebrugge (model run HSW113_K17a).

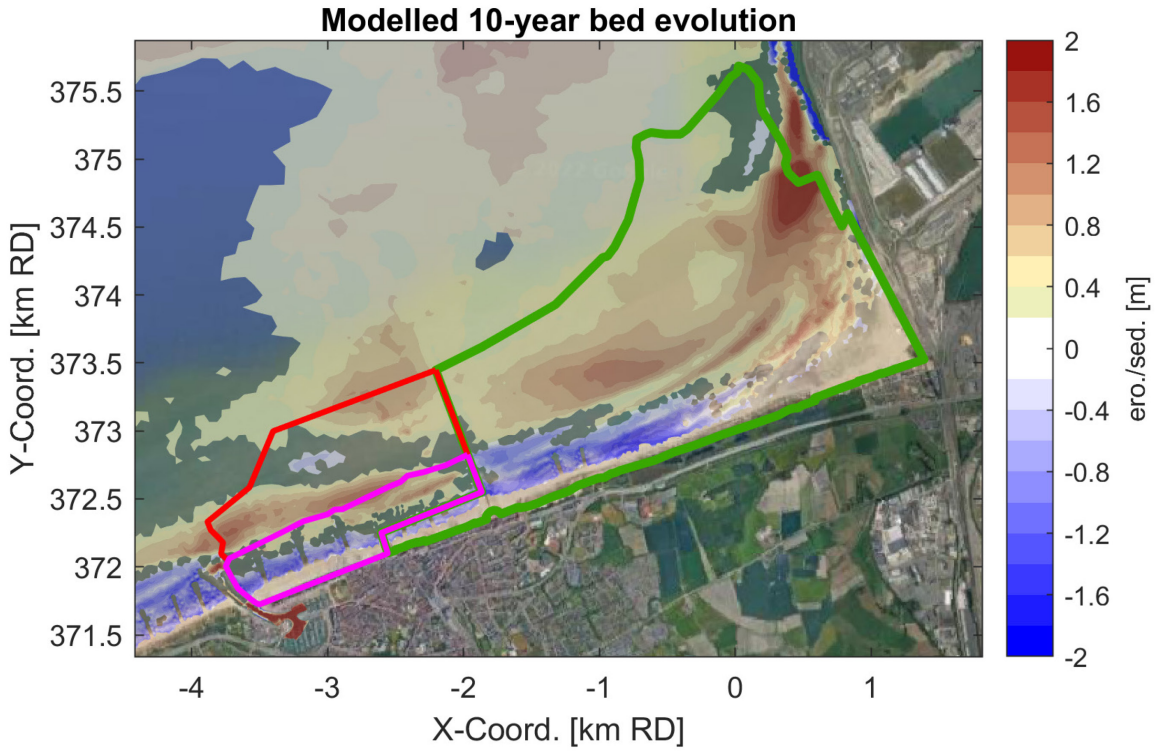


Figure 13: Modelled ten-year bed evolution using Wu & Lin formula, bedload equation and ten fractions without cross-shore sediment transport, in the area next to the western dam of Zeebrugge (HSW113_S05b).

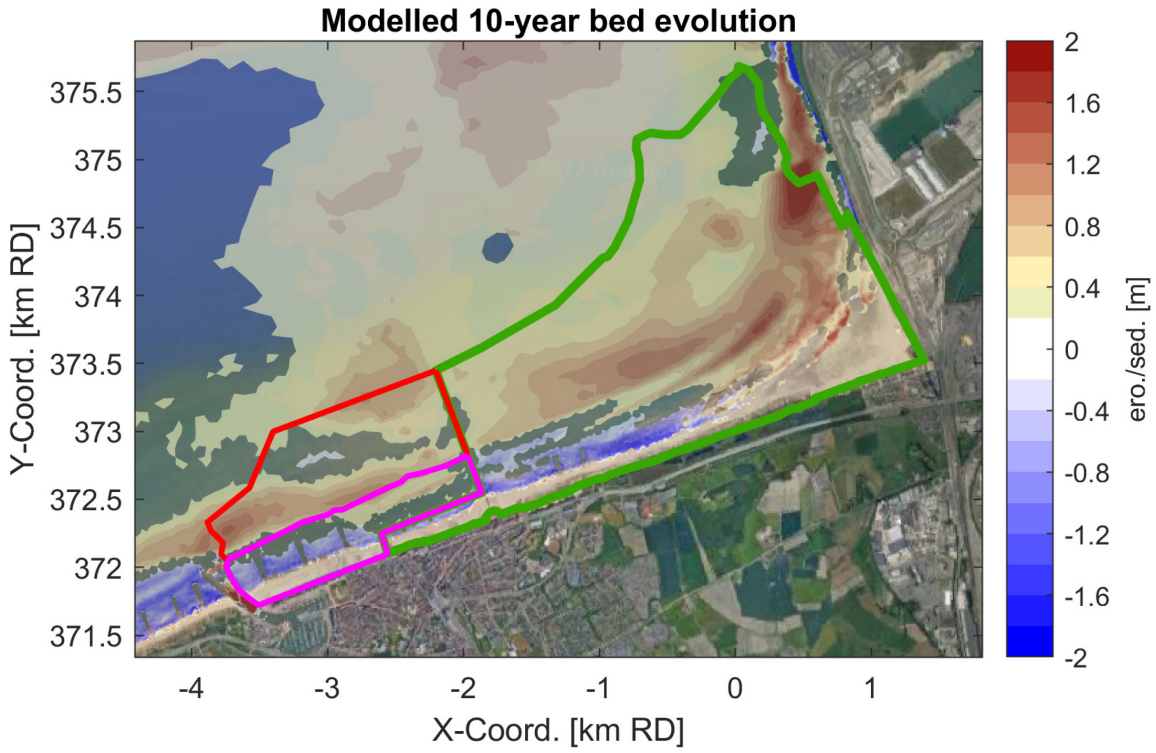


Figure 14: Modelled ten-year bed evolution using Wu & Lin formula, advection-diffusion equation and ten fractions without cross-shore sediment transport, in the area next to the western dam of Zeebrugge (HSW113_S06c).

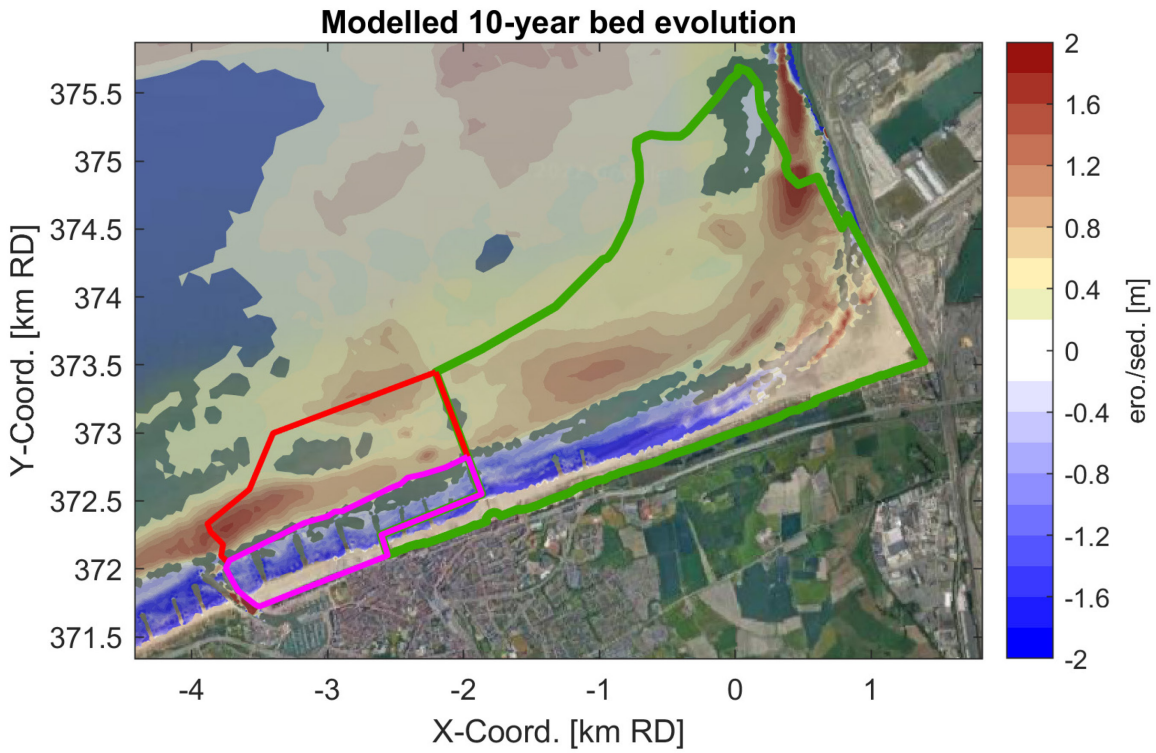


Figure 15: Modelled ten-year bed evolution using Wu & Lin formula, advection-diffusion equation and ten fractions with cross-shore sediment transport, in the area next to the western dam of Zeebrugge (HSW113_S06a).

Table 2: Comparison between measured and modelled net volume change within different polygons for the validation case: bed evolution next to the Western dam of Zeebrugge.

	Net volume change (m^3/y) in		
	Green polygon	**Red polygon**	**Pink polygon**
Verwaest et al., 2011	370,000	35,000	-5,000
Bijker, toal-load, two fractions, without CST (HSW113_K17a)	240,000 -35%	73,000 +109%	7,000 -240%
Wu & Lin, toal-load, ten fractions, without CST (HSW113_S05b)	227,000 -39%	57,000 +63%	1,200 -124%
Wu & Lin, advection-diffusion, ten fractions, without CST (HSW113_S06c)	258,000 -30%	63,000 +80%	-6,300 +26%
Wu & Lin, advection-diffusion, ten fractions, with CST (HSW113_S06a)	172,000 -54%	78,000 +123%	-37,000 +640%

3.2 Erosion in front of Wenduine

The objective of this case study is to validate the performance of the model on medium-long time scales (one year) for a situation where longshore sediment transport is important.

The morphological model was run with brute force wave and wind conditions in combination with real spring-neap tidal forcing during the period between 01 June 2014 and to 01 June 2015. The spring-neap tidal boundaries were obtained from nesting with the regional ZUNO model (Maximova *et al.*, 2016). The modelled bed evolution was validated with net volume change in the closed pink box along the coast (Figure 16). The period is characterised by strong erosion of the recently nourished foreshore and beach nourishment at Wenduine.

Figure 17 - Figure 20 displays the modelled morphological change over one year with the four different settings. The observed morphological change was calculated based on the difference between lidar and foreshore surveys of spring 2014 and spring 2015 (Figure 16). All four settings successfully reproduce the pronounced erosion in front of Wenduine, as the initial bathymetry (spring 2014) includes a recent nourishment executed in February-March 2014.

Table 3 presents a comparison between the measured net erosion and the modelled results obtained using different settings for the sediment transport. The measured net erosion amounts to 146,000 m³ (Figure 16). The simulation using the Bijker bedload formulation with two sediment fractions (without CST) shows excellent agreement with the measurements, with an overestimation of only 0.34% (Figure 17), while the formulations by Wu & Lin without CST underestimate the erosion by 15.68% for the bedload approach (Figure 18) and 14.04% for the advection–diffusion approach (Figure 19). When CST is included in the Wu & Lin advection–diffusion model, the results are improved slightly, reducing the underestimation to 6.58% (Figure 20). In this validation case, the Bijker formulation provides the best agreement with the measured net erosion volume. However, a visible discrepancy remains in the cross-shore distribution of erosion. Compared to the model results obtained with all four settings, the measured erosion takes place in the nearshore zone, whereas the modelled erosion is located further offshore. This indicates that the model fails to reproduce erosion processes in relatively shallow areas.

A more detailed investigation reveals that the modelled erosion is limited to elevations below approximately 4 m TAW, while the measured erosion extends to the area above 6 m TAW. Notably, the maximum water level during the simulation reaches about 5.8 m TAW, which suggests that the observed nearshore erosion cannot be fully explained by the water level alone. Therefore, infragravity waves are likely to play a significant role in the observed erosion in the shallow zone, which are not included in the current model setup.

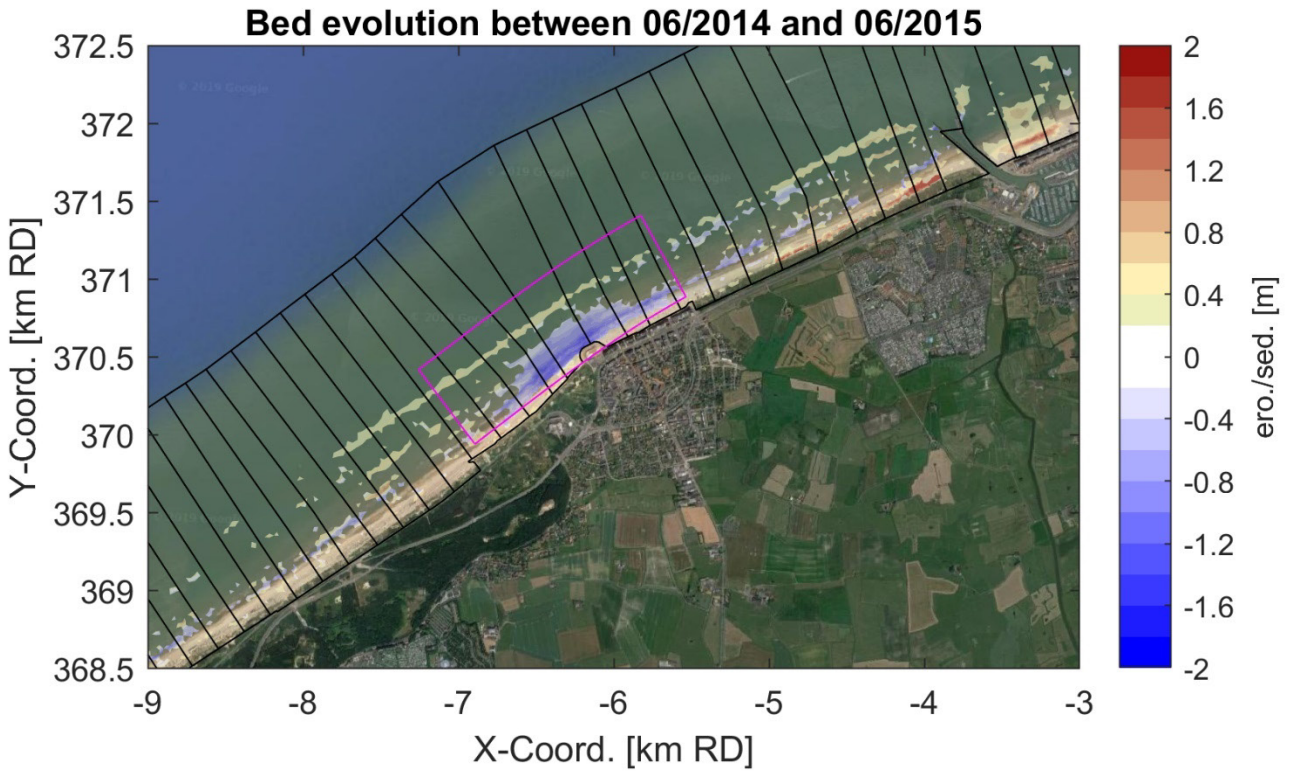


Figure 16: Measured one-year morphological change at Wenduine.

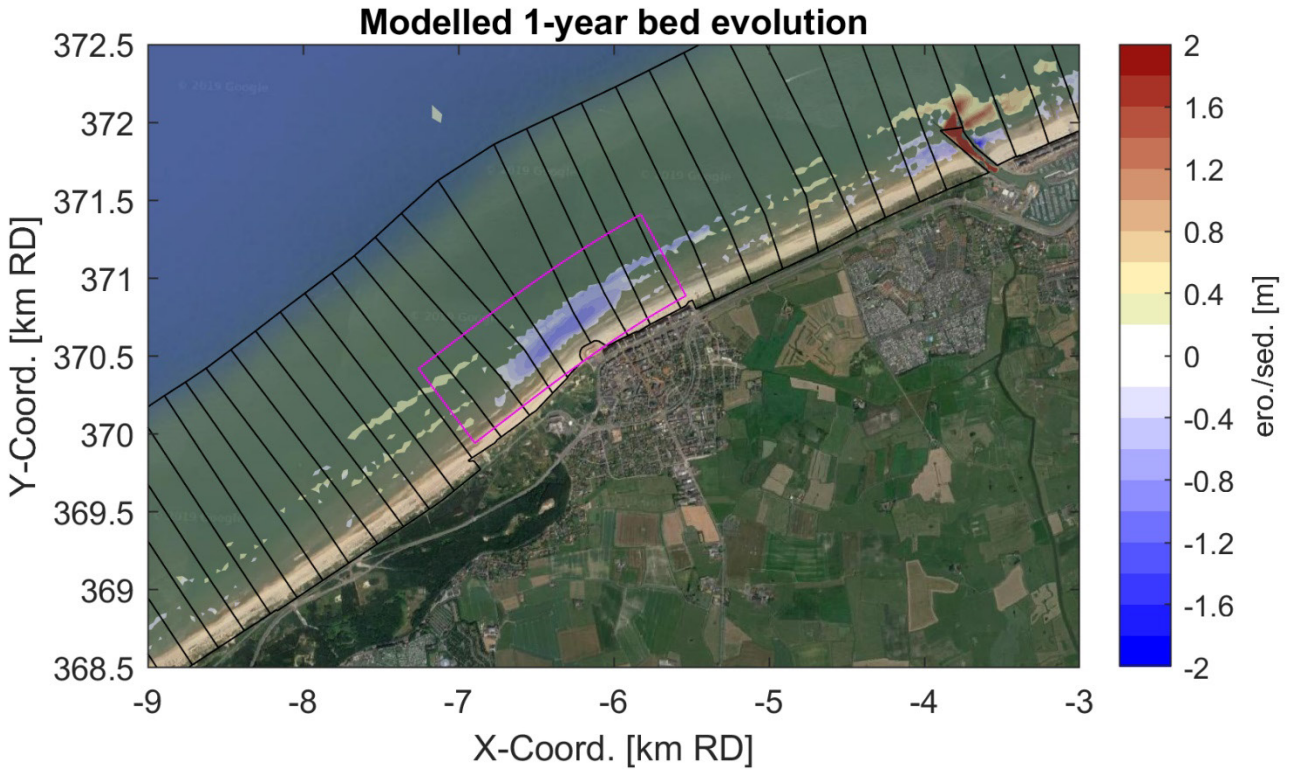


Figure 17: Modelled one-year morphological change at Wenduine, using Bijker formula, bedload equation and two fractions without cross-shore sediment transport.

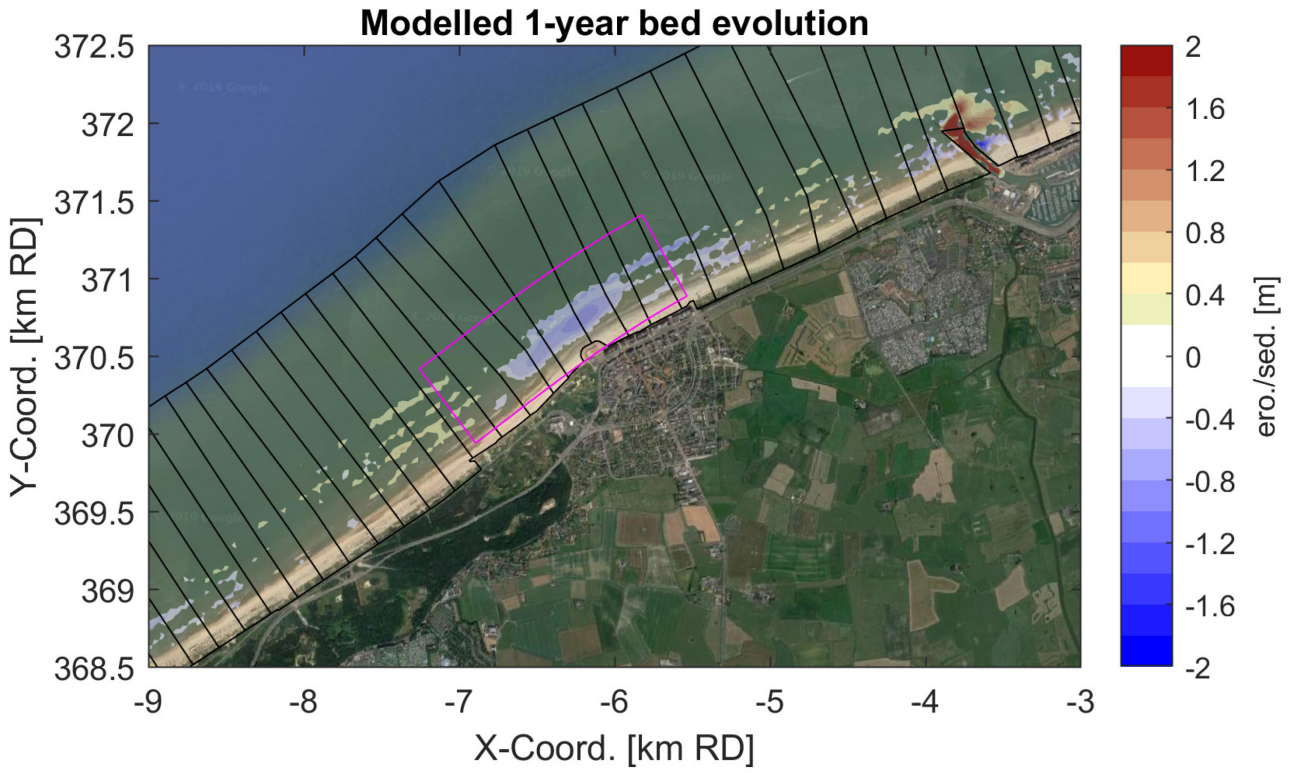


Figure 18: Modelled one-year morphological change at Wenduine, using Wu & Lin formula, bedload equation and ten fractions without cross-shore sediment transport.

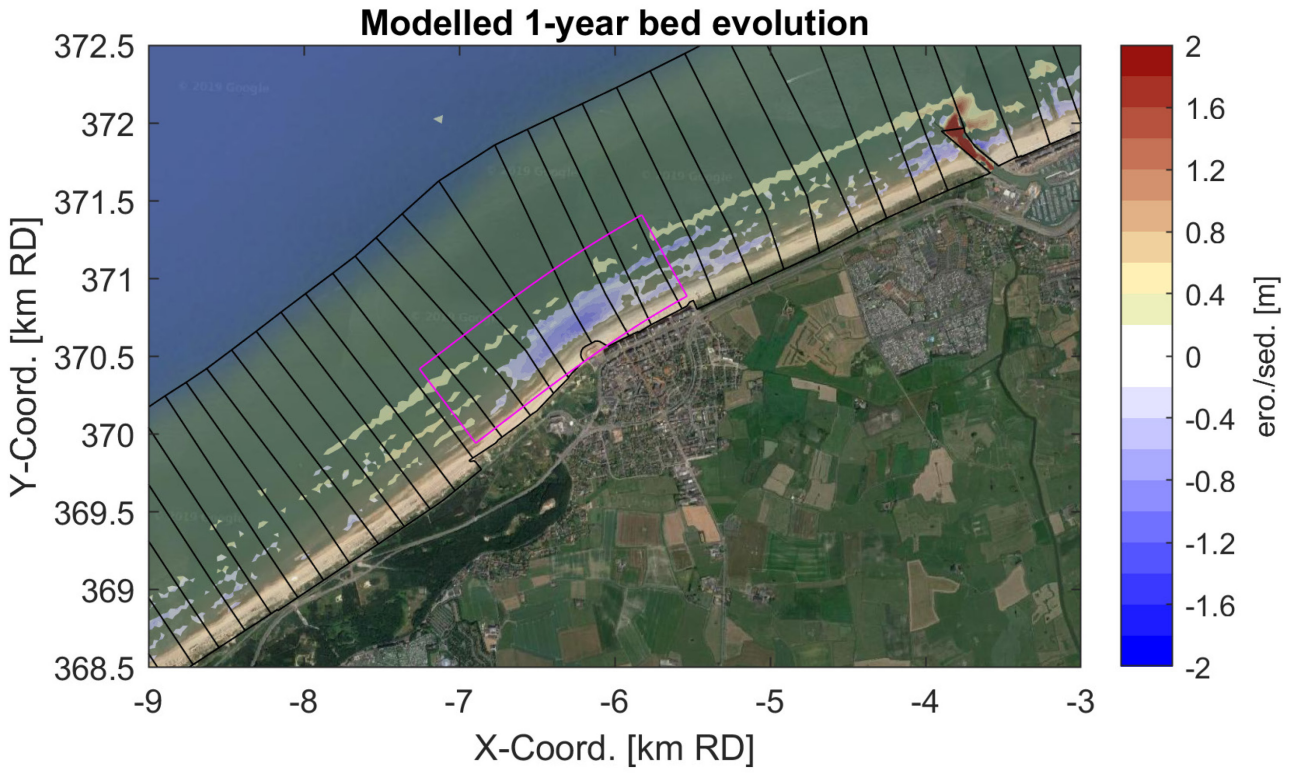


Figure 19: Modelled one-year morphological change at Wenduine, using Wu & Lin formula, advection-diffusion equation and ten fractions without cross-shore sediment transport.

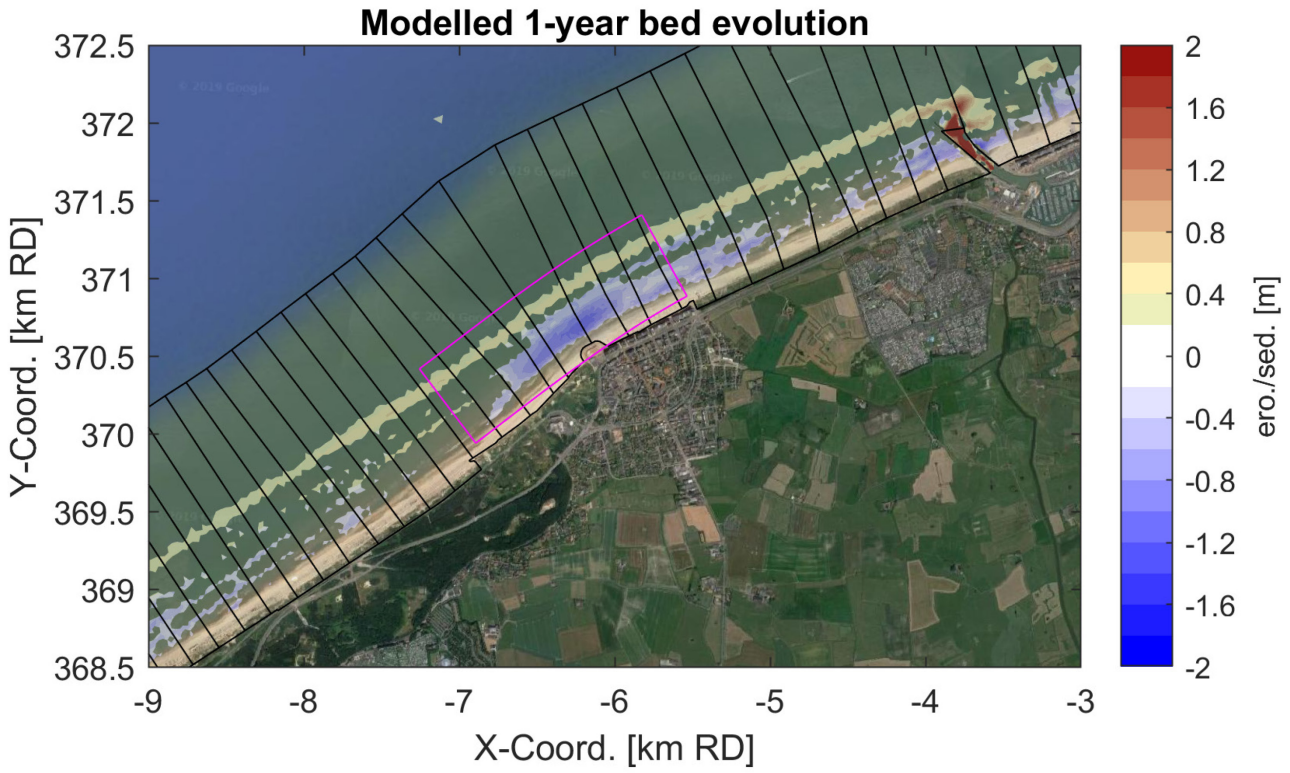


Figure 20: Modelled one-year morphological change at Wenduine, using Wu & Lin formula, advection-diffusion equation and ten fractions with cross-shore sediment transport.

Table 3: Comparison between measured and modelled net erosion in front of Wenduine.

	Net erosion (m^3)
Measurement	146,000
Bijker, total-load, two fractions, without CST (HSW015b_C04)	146,500; 0.34%
Wu & Lin, total-load, ten fractions, without CST (HSW015b_D05a and HSW015b_D05b)	123,100; -15.68%
Wu & Lin, advection-diffusion, ten fractions, without CST (HSW015b_D04c and HSW015b_D04d)	125,500; -14.04%
Wu & Lin, advection-diffusion, ten fractions, with CST (HSW015b_D03c and HSW015b_D03d)	136,400; -6.58%

3.3 Annual sedimentation at Blankenberge

The objective of this test is to validate the performance of the model on medium-long time scales (one year) for a situation where longshore sediment transport is important.

In addition to the constant structural erosion occurring at Wenduine, the port of Blankenberge experiences strong sedimentation in its entrance channel requiring frequent dredging. In order to capture the wave characteristics more accurately within the entrance channel, where significant sedimentation occurs, the wave mesh was refined in the port area and aligned with the flow mesh (pink lines in Figure 21). The same representative half year used for the Zeebrugge validation case (Section 3.1) was adopted for this validation case, using a morphological acceleration factor (MorFac) of 2 to simulate the annual sedimentation in the port.

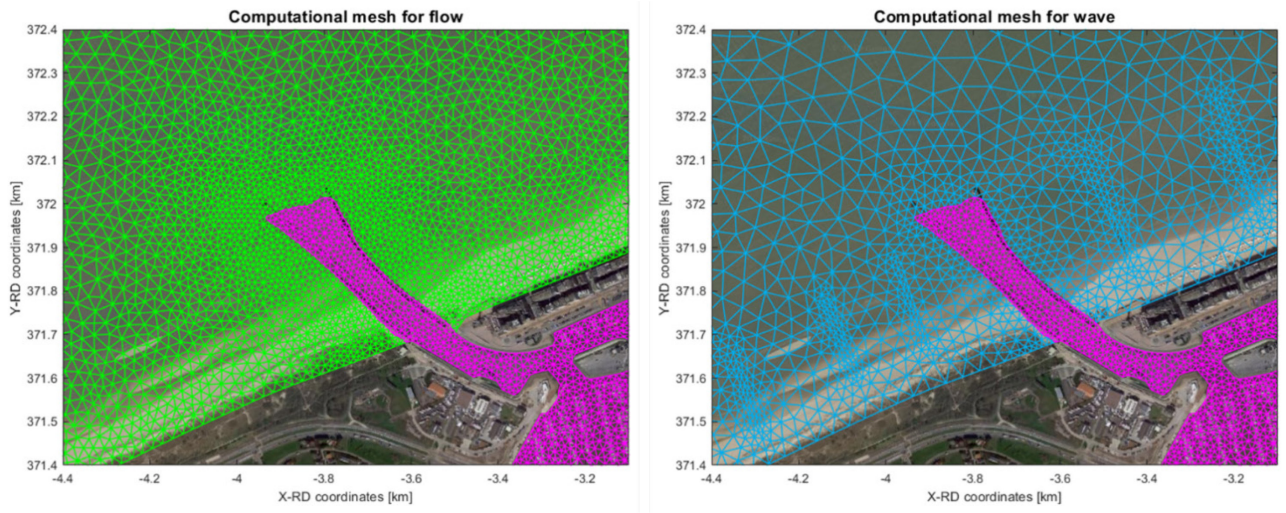


Figure 21: Flow (left) and wave (right) meshes in area around Blankenberge.

Figure 22 presents the estimated sedimentation pattern derived from dredging volumes over the period 1980–2010. Figure 23 - Figure 26 show the modelled bed evolution over one year for four different model settings. The modelled sedimentation was computed within the dashed polygon, and the corresponding values are summarized in Table 5.

Table 4: Overview of the model settings used for the validation of annual sedimentation at Blankenberge.

Run ID	Transport formulation	Transport approach	Sediment fractions	CST
HSW071_D13	Bijker	Total-load	2	No
HSW071_F06	Wu & Lin	Total-load	10	No
HSW071_F08	Wu & Lin	Advection–diffusion	10	No
HSW071_F07	Wu & Lin	Advection–diffusion	10	Yes

A comparison between the dredging-based estimates and the model results indicates that the spit-shaped sedimentation pattern is reasonably well reproduced. However, all models underestimate the sedimentation in front of the channel entrance (zone A in Figure 22).

Differences between the transport formulations are also visible. Compared to the Bijker formulation (Figure 23), the Wu & Lin formulation (Figure 24) produces a more landward-extended accretion zone. This landward extension becomes even more pronounced when the advection-diffusion equation is used for the sediment transport (Figure 25 and Figure 26).

Table 5 compares the simulated gross sedimentation rates obtained with the different model settings against the reference value reported by Teurlinx et al. (2009), which amounts to 165,000 m^3/y. All model settings yield results within a relatively narrow range (161,000–181,000 m^3/y), corresponding to deviations between −2.4% and +9.7% from the reference value. This suggests that the model is generally capable of reproducing the gross sedimentation rates with reasonable accuracy.

The Bijker bedload formulation with two sediment fractions shows the largest overestimation (+9.7%), whereas the Wu & Lin bedload formulation with ten sediment fractions yields a slight underestimation (−2.4%), providing the closest agreement with the reference. The Wu & Lin advection-diffusion formulation results in a slight overestimation (+2.4%), while the inclusion of CST leads to a larger overestimation (approximately +10%), although the overall differences remain limited.

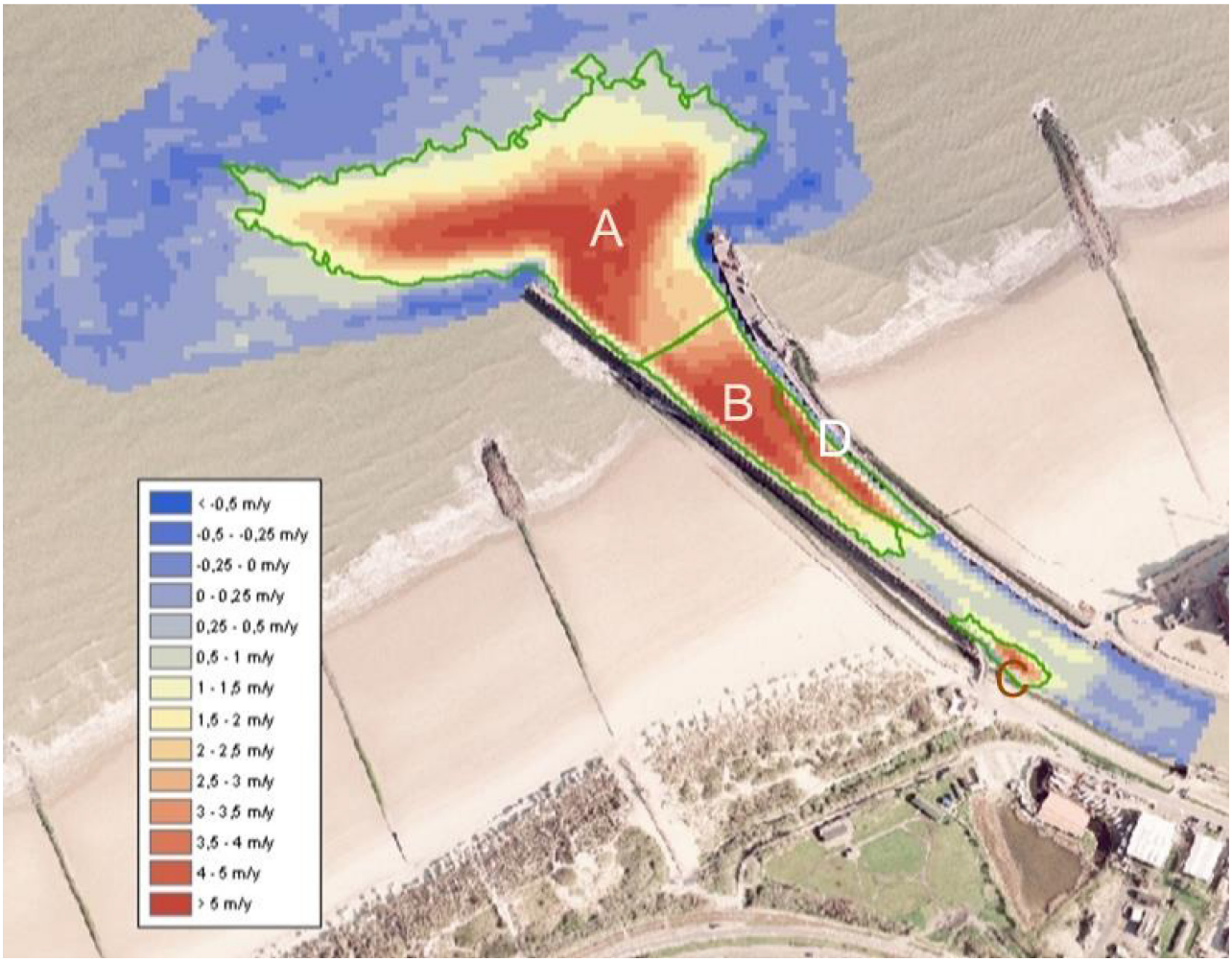


Figure 22: Estimated annual sedimentation in the entrance channel for the port of Blankenberge (reproduced from Teurlincx et al., 2009).

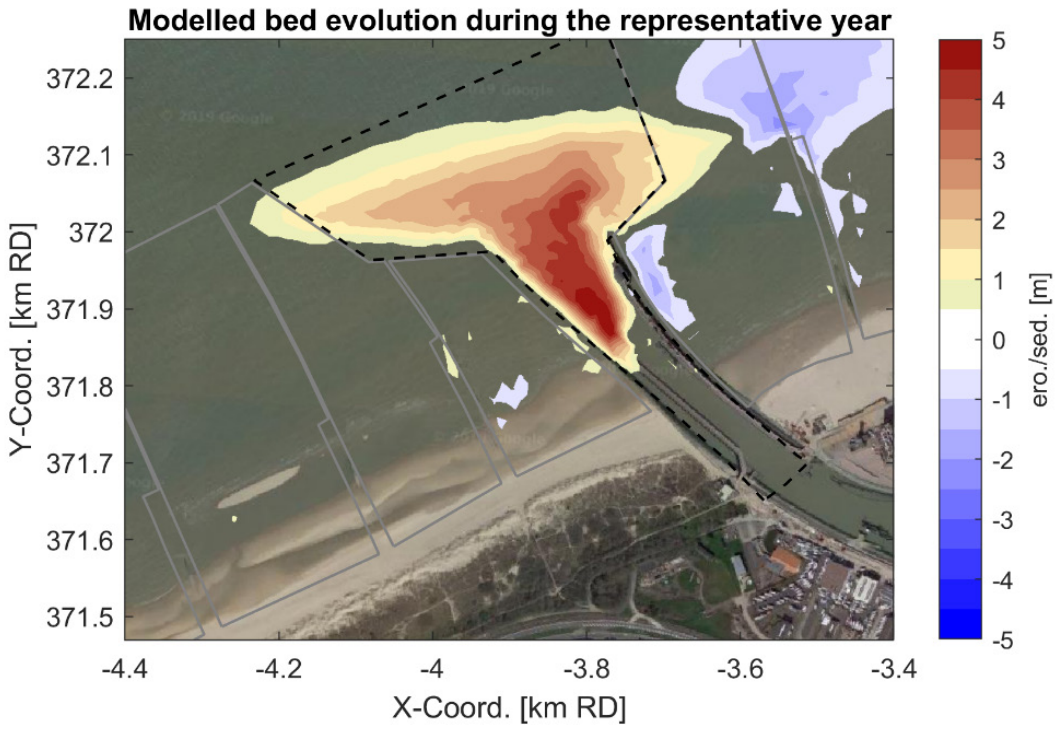


Figure 23: Modelled 1-year bed evolution with representative tide and wave/wind over a half year (MorFac =2), in the area around the port of Blankenberge, using Bijker formula, bedload equation and two fractions without cross-shore sediment transport.

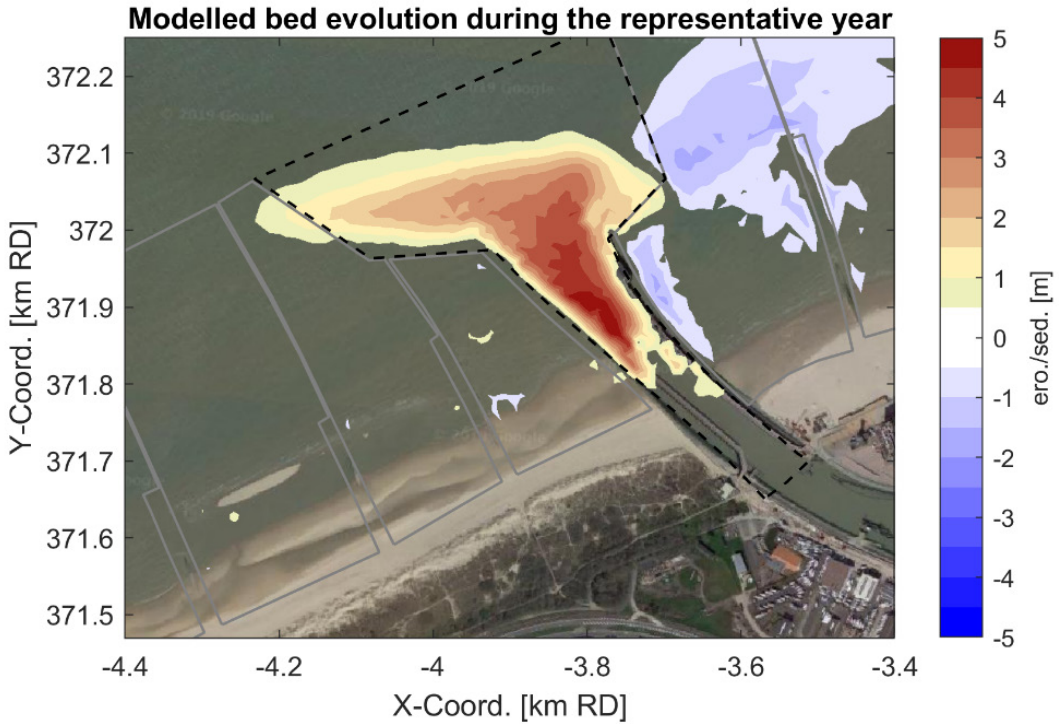


Figure 24: Modelled 1-year bed evolution with representative tide and wave/wind over a half year (MorFac =2), in the area around the port of Blankenberge, using Wu & Lin formula, bedload equation and ten fractions without cross-shore sediment transport.

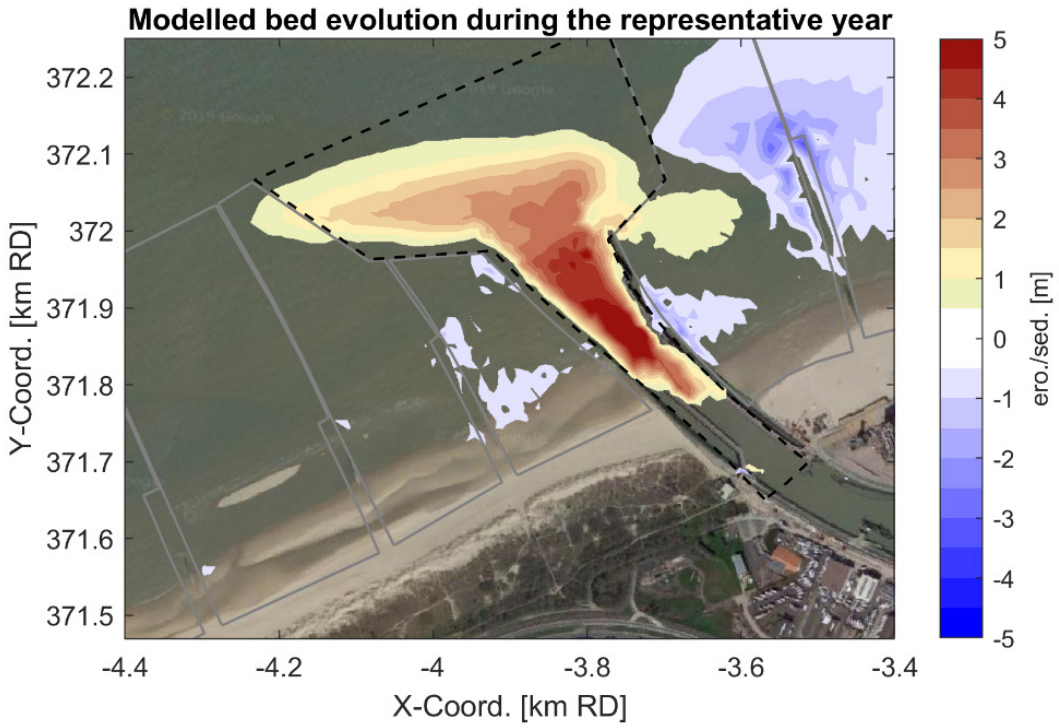


Figure 25: Modelled 1-year bed evolution with representative tide and wave/wind over a half year (MorFac =2), in the area around the port of Blankenberge, using Wu & Lin formula, advection-diffusion equation and ten fractions without cross-shore sediment transport.

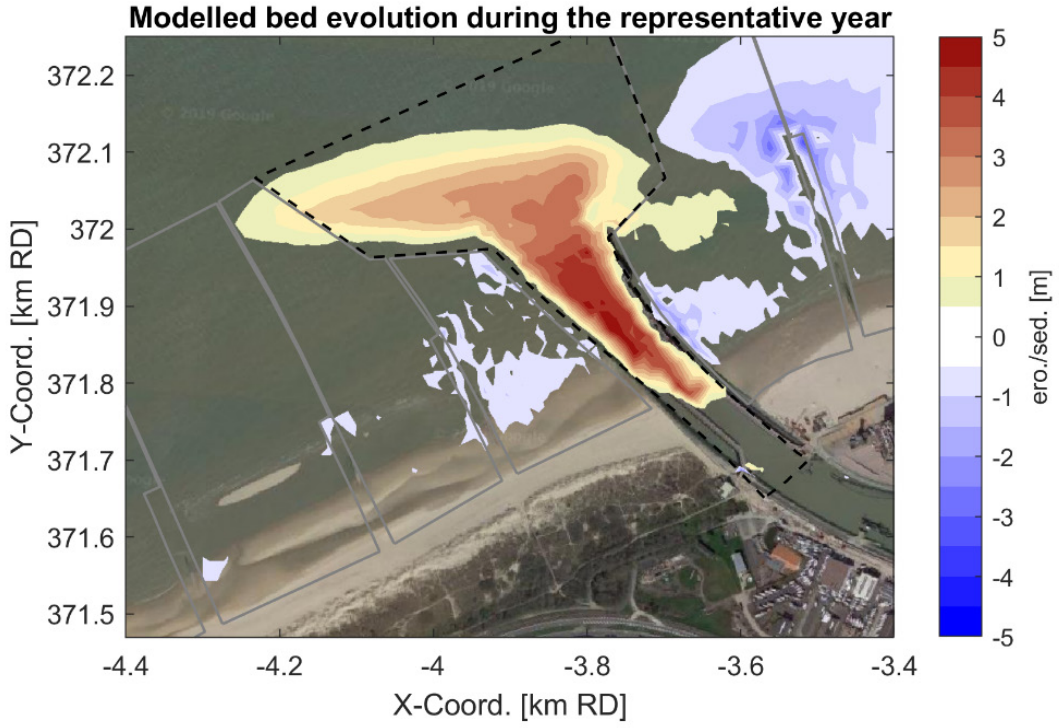


Figure 26: Modelled 1-year bed evolution with representative tide and wave/wind over a half year (MorFac =2), in the area around the port of Blankenberge, using Wu & Lin formula, advection-diffusion equation and ten fractions with cross-shore sediment transport.

Table 5: Comparison between measured and modelled annual sedimentation at Blankenberge.

	Gross sedimentation (m^3/y)
Teurlinx et al., 2009	165,000
Bijker, total-load, two fractions, without CST (HSW071_D13)	181,000; +9.7%
Wu & Lin, total-load, ten fractions, without CST (HSW071_F06)	161,000; -2.4%
Wu & Lin, advection-diffusion, ten fractions, without CST (HSW071_F08)	169,000; +2.4%
Wu & Lin, advection-diffusion, ten fractions, with CST (HSW071_F07)	175,000; +6.1%

3.4 Storm-induced siltation at Blankenberge

The objective of this validation case is to assess the capability of the model to reproduce short-term morphodynamic behaviour during a storm event for a situation where alongshore sediment transport is the main physical process leading to sedimentation in an entrance channel.
The storm Ciara (February 2020) provides a suitable case for further validation of the morphological model. Bathymetric surveys of the port of Blankenberge were conducted on 6 and 14 February 2020, respectively before and after the storm. The bed evolution during the storm was derived from these two surveys (Figure 27). All four model settings were also applied to this validation case (Table 6). As shown in Figure 28 - Figure 31, all four settings successfully reproduce a similar spit-shaped sedimentation pattern formed during the storm (Figure 28 - Figure 31).

Table 6: Overview of the model settings used for the validation of storm-induced siltation at Blankenberge.

Run ID	**Transport formulation**	**Transport approach**	**Sediment fractions**	**CST**
HSW113_L09	Bijker	Total-load	2	No
HSW113_L30c	Wu & Lin	Total-load	10	No
HSW113_L31e	Wu & Lin	Advection–diffusion	10	No
HSW113_L31d	Wu & Lin	Advection–diffusion	10	Yes

A quantitative comparison is presented in Table 7. The measurement indicates a total net volume increase of 4.36×10^4 m³, calculated as the sum of erosion (negative) and sedimentation (positive) volumes, and a gross volume change of 4.77×10^4 m³, calculated as the sum of the absolute sedimentation volume. All model settings reproduce the correct order of magnitude of the total volume change, although noticeable differences exist in the spatial distribution between the approach area and the channel.

The Bijker formulation overestimates the total volume change by approximately 27% (net) and 17% (gross), whereas all Wu & Lin-based formulations underestimate the total volume change, with deviations ranging from approximately −5% to −11% (net). Overall, the sediment budget is reasonably captured by all transport formulations, although the magnitude of the predicted changes is sensitive to the choice of transport formulation.

A major discrepancy is observed in the approach area:

- The measurement indicates substantial accretion (net: 2.7×10^4 m³; gross: 3.0×10^4 m³);
- All model settings significantly underestimate sedimentation, with deviations ranging from −10% (Bijker) to approximately −50% (Wu & Lin formulations).

In contrast, the channel exhibits an opposite trend:

- The measured sedimentation is relatively modest (net: 1.6×10^4 m³; gross: 1.8×10^4 m³);
- All model settings substantially overestimate sedimentation, with deviations ranging from 46% to 88% (net values).

The Bijker formulation provides the closest agreement in the approach area but significantly overestimates sedimentation in the channel. The Wu & Lin bedload formulation results in a larger underestimation in the approach area, but a smaller overestimation in the channel. The advection - diffusion transport formulation slightly improves the spatial distribution, although the discrepancy remains. The inclusion of CST has only a minor effect on both the overall sediment budget and the spatial distribution.

The underestimation of sedimentation in the approach area may be related to the bathymetric data applied in the model. Outside the black dashed polygons, the bathymetry is based on a survey conducted in early 2019, approximately one year prior to the storm event. In contrast, the overestimation in the channel may be associated with the presence of piles located along both sides of the channel (Figure 32). These structures are not explicitly included in the model due to their small scale relative to the mesh resolution. However, the relatively high density of piles, including locations with double rows, is likely to induce significant flow resistance, thereby reducing sediment transport in reality.

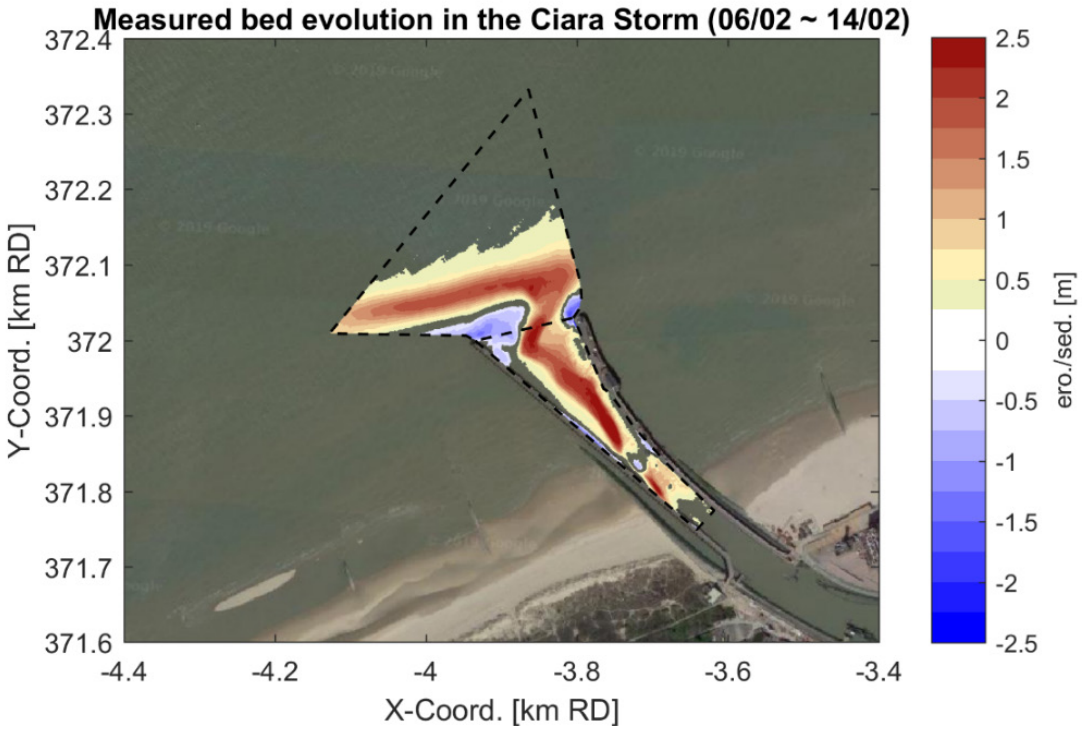


Figure 27: Measured sedimentation in the entrance channel for the port of Blankenberge during the Ciara Storm.

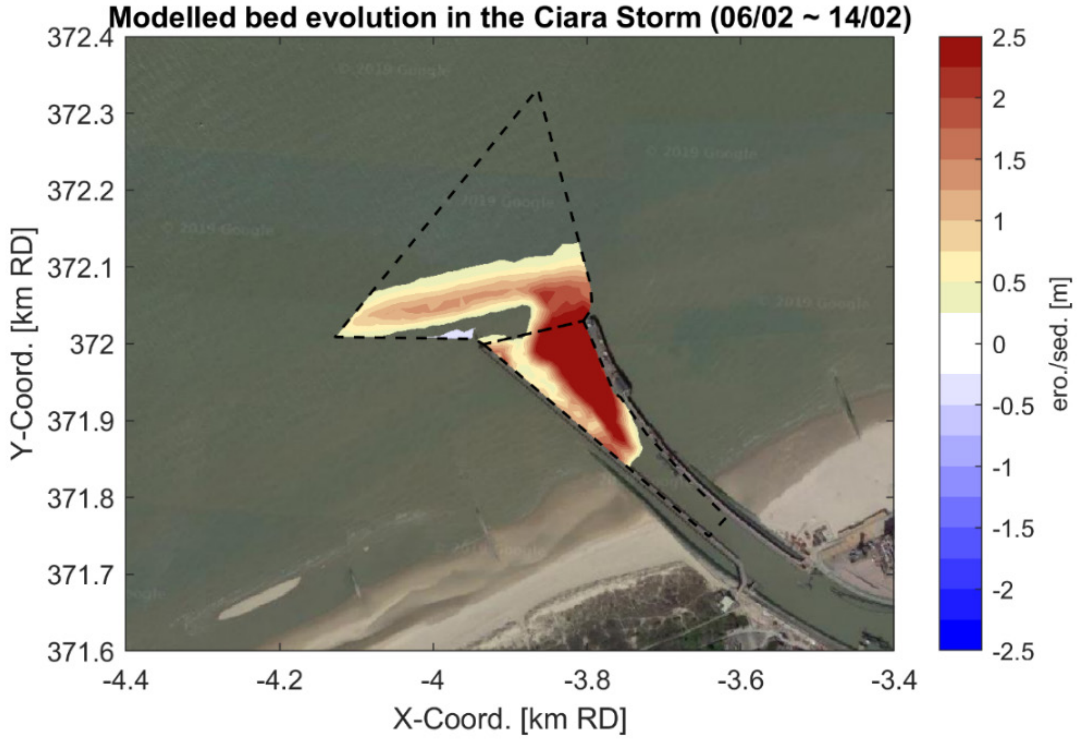


Figure 28: Modelled sedimentation in the entrance channel for the port of Blankenberge during the Ciara Storm, using Bijker formula, bedload equation and two fractions without cross-shore sediment transport.

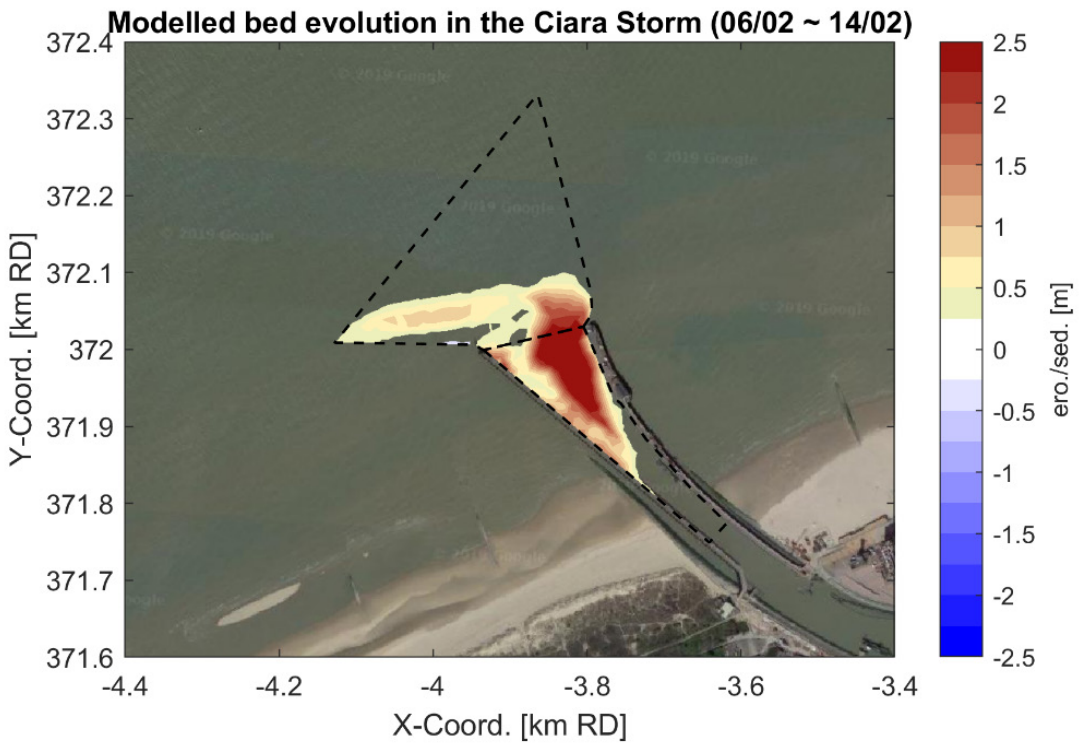


Figure 29: Modelled sedimentation in the entrance channel for the port of Blankenberge during the Ciara Storm, using Wu & Lin formula, bedload equation and ten fractions without cross-shore sediment transport.

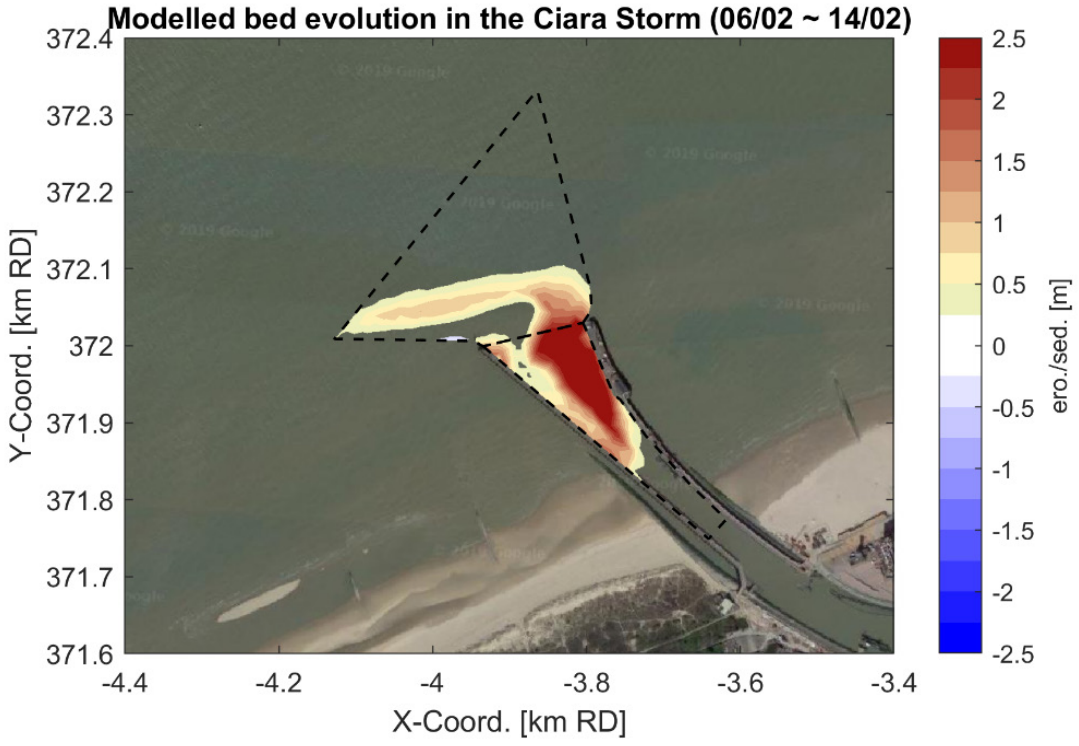


Figure 30: Modelled sedimentation in the entrance channel for the port of Blankenberge during the Ciara Storm, using Wu & Lin formula, advection-diffusion equation and ten fractions without cross-shore sediment transport.

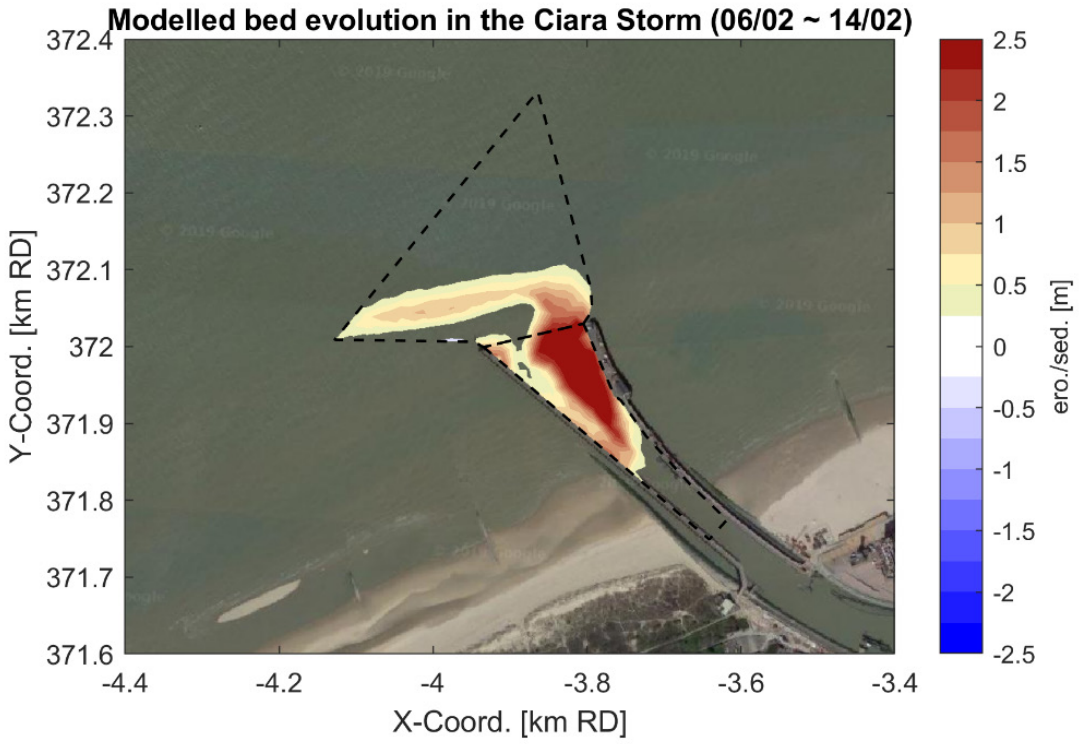


Figure 31: Modelled sedimentation in the entrance channel for the port of Blankenberge during the Ciara Storm, using Wu & Lin formula, advection-diffusion equation and ten fractions with cross-shore sediment transport.

Table 7: Comparison between measured and modelled net and gross volume changes within separated zones for the validation case: storm-induced siltation at Blankenberge.

	Volume change (m^3) in Voorplein		**Volume change (m^3) in Geul**		**Total volume change (m^3)**	
	Net	Gross	Net	Gross	Net	Gross
Measurement	2.71E+04	2.98E+04	1.65E+04	1.79E+04	4.36E+04	4.77E+04
Bijker, total-load, two fractions, without CST (HSW113_L09)	2.44E+04 -10.0%	2.49E+04 -16.4%	3.10E+04 87.9%	3.10E+04 73.2%	5.54E+04 27.1%	5.59E+04 17.2%
Wu & Lin, total-load, ten fractions, without CST (HSW113_L30c)	1.45E+04 -46.56%	1.48E+04 -50.34%	2.41E+04 46.26%	2.42E+04 34.97%	3.86E+04 -11.43%	3.90E+04 -18.33%

Wu & Lin, advection-diffusion, ten fractions, without CST (HSW113_L31e)	1.39E+04 -48.87%	1.43E+04 -52.08%	2.70E+04 63.42%	2.70E+04 50.80%	4.08E+04 -6.38%	4.13E+04 -13.48%
Wu & Lin, advection-diffusion, ten fractions, with CST (HSW113_L31d)	1.50E+04 -44.57%	1.53E+04 -48.51%	2.65E+04 60.69%	2.65E+04 48.28%	4.15E+04 -4.74%	4.19E+04 -12.19%



Figure 32: Piles located along both sides of the entrance channel at Blankenberge port.

4 Conclusions

This study presents the evaluation and validation of updated sediment transport formulations within the ScaldisCoast modelling framework. The results demonstrate that the model is capable of reproducing the general magnitude and the spatial patterns of morphological change across a range of temporal scales, from storm events to long-term coastal evolution.

The comparison of sediment transport formulations shows that both the Bijker and Wu & Lin formulations produce comparable orders of magnitude in sediment transport rates. However, the Bijker formulation exhibits a strong sensitivity to the fine sediment fraction (D_{50}: 100 µm) in the schematised model tests. The Wu & Lin formulation, combined with a multi-fraction sediment representation, provides a more physically realistic description of sediment behaviour by accounting for hiding and exposure effects. Moreover, this multi-fraction approach decouples sediment composition from the transport formulation, resulting in a more generic and flexible modelling framework.

The implementation of the advection-diffusion approach produces transport predictions comparable to those of the traditional bedload formulation, while enabling the inclusion of cross-shore transport processes. However, the inclusion of cross-shore transport (CST) evidently affects the spatial distribution of sedimentation and erosion and may in some cases lead to overestimation or unrealistic sediment redistribution.

The validation cases highlight a few key findings below:

- The model successfully reproduces wave-driven alongshore sediment transport and associated morphological patterns;
- The overall sediment budget is generally well captured across all cases;
- Significant discrepancies remain in the spatial distribution of sedimentation and erosion, particularly in complex environments such as harbour entrance channels;
- Nearshore processes, such as infragravity waves and small-scale structures (e.g. piles), are not yet represented and may contribute to local mismatches between results and observations.

Among the tested settings, the new model release combines the Wu & Lin formulation with multi-fraction sediment and advection-diffusion transport, providing a generic and flexible framework. Nevertheless, no single setting consistently outperforms the others across all validation cases.

Overall, the updated ScaldisCoast model demonstrates good performance in the modelling of coastal morphodynamics along the Belgian coast. Further improvements are recommended, particularly in the representation of infragravity waves and small-scale structures. In addition, extending the current cross-shore sediment transport formulation to a three-dimensional (3D) approach could provide a more realistic representation of cross-shore sediment dynamics and further enhance the predictive capability of the model.

Model input files of the validation testcases haven been added to the model SVN repository:

- https://wl-subversion.vlaanderen.be/!/#repoSpNumMod/view/head/TELEMAC/Scaldis-Kust/21_104%20Release%20Scaldis-Kust%202026

References

Bijker, E.W. (1971). Longshore transport computations. *Journal of the Waterways, Harbors and Coastal Engineering Division, 97,* 687-701.

Fonias, E., Breugem, W.A., Wang, L., Bolle, A., Kolokythas, G., & De Maerschalck, B. (2021). Implementation of cross-shore processes in GAIA. *In Proceedings of the papers submitted to the 2020 TELEMAC-MASCARET user conference - October 2021* (pp. 138–143).

Kolokythas, G., De Maerschalck, B., Wang, L., Fonias, S., Breugem, W. A., Vanlede, J., & Mostaert, F. (2021). *Modelling Belgian Coastal zone and Scheldt mouth area Modelling Belgian Coastal zone and Scheldt mouth area Sub report 12: Scaldis-Coast model – Model setup and validation of the 2D hydrodynamic model.*

Kolokythas, G.; Breugem, W.A.; Wang, L.; De Maerschalck, B. (2024). Advances in cross-shore transport modelling with GAIA. *In Proceedings of the XXXth TELEMAC Users Conference, 8-9 October 2024* (pp. 1–10).

Open Telemac-Mascaret. (2019). *GAIA User manual. Accessed from http://wiki.opentelemac.org/.*

Soulsby, R.(1997). *Dynamics of marine sands, a manual for practical applications. Thomas Telford, London.*

Teurlincx, R., van der Biest, K., Reyns, J., Verwaest, T., & Mostaert, F. (2009). *Haven Van Blankenberge - Verminderen van de aanzanding van de havengeul en het voorplein: Eindrapport (Dutch). Versie 11. WL Rapporten, 643 12. Waterbouwkundig Laboratorium: Antwerpen, België.*

van Rijn, L.C. (1993). *Principles of Sediment Transport in Rivers, Estuaries and Coastal Seas. Aqua Publications, The Netherlands.*

van Rijn, L.C. (2007). Unified View of Sediment Transport by Currents and Waves. II: Suspended Transport. *Journal of Hydraulic Engineering, 133(6),* 668–689.

Verwaest, T.; Delgado, R.; Janssens, J.; Reyns, J. (2011). Longshore sediment transport along the Belgian coast. *in: Coastal sediments 2011: "Bringing Together Theory and Practice", May 2-6, Hyatt Regency Miami, Miami, Florida, USA: proceedings* (pp. 1528-1538).

Wang, L.; Kolokythas, G.; Breugem, W.A.; De Maerschalck, B. (2026). *Modelling Belgian Coast: ScaldisCoast: Sub report 2 – Updates ScaldisCoast 2025. Version 4.0. FH Reports, 21_104_2. Flanders Hydraulics: Antwerp.*

Wu, W., Lin, Q. (2014). Nonuniform sediment transport under non-breaking waves and currents. *Coastal Engineering, 90,* 1-11.

Appendix A Coupled model settings for TELEMAC version v8p4

A.1 Settings of TELEMAC-2D module

Table A-1: Hydrodynamic model settings for Series A and B.

Parameter	**Setting**
TIME STEP	6
COUPLING PERIOD FOR TOMAWAC	300
LAW OF BOTTOM FRICTION	4
FRICTION COEFFICIENT	0.02
TURBULENCE MODEL	4
VELOCITY DIFFUSIVITY	1
WAVE DRIVEN CURRENTS	YES
WIND	YES
OPTION FOR WIND	2
CORIOLIS	YES
CORIOLIS COEFFICIENT	1.14E-04
TIDAL FLATS	YES
OPTION FOR THE TREATMENT OF TIDAL FLATS	1
ADVECTION	YES
NUMBER OF SUB-ITERATIONS FOR NON-LINEARITIES	1
PROPAGATION	YES
FREE SURFACE GRADIENT COMPATIBILITY	0.9
IMPLICITATION FOR DEPTH	0.6
IMPLICITATION FOR VELOCITY	0.6
INITIAL GUESS FOR H	1
TREATMENT OF THE LINEAR SYSTEM	2
MATRIX STORAGE	3
TREATMENT OF NEGATIVE DEPTHS	1
SOLVER ACCURACY	1.00E-05
SOLVER	7
SOLVER OPTION	5
MAXIMUM NUMBER OF ITERATIONS FOR SOLVER	300
MASS-LUMPING ON H	1
CONTINUITY CORRECTION	YES
MASS-LUMPING ON VELOCITY	0

SUPG OPTION	0;1
DISCRETIZATIONS IN SPACE	11;11
TYPE OF ADVECTION	1;5

Table A-2: Hydrodynamic model settings for Series C and D.

Parameter	**Setting**
TIME STEP	6
COUPLING PERIOD FOR TOMAWAC	300
LAW OF BOTTOM FRICTION	4
FRICTION COEFFICIENT	0.02
TURBULENCE MODEL	4
VELOCITY DIFFUSIVITY	1
WAVE DRIVEN CURRENTS	YES
WIND	YES
OPTION FOR WIND	2
CORIOLIS	YES
CORIOLIS COEFFICIENT	1.14E-04
TIDAL FLATS	YES
OPTION FOR THE TREATMENT OF TIDAL FLATS	1
DIFFUSION OF TRACERS	NO
FREE SURFACE GRADIENT COMPATIBILITY	0.9
IMPLICITATION FOR DEPTH	1.0
INITIAL GUESS FOR H	1
TREATMENT OF THE LINEAR SYSTEM	2
MATRIX STORAGE	3
TREATMENT OF NEGATIVE DEPTHS	3
SOLVER ACCURACY	1.00E-05
SOLVER	7
SOLVER OPTION	5
MAXIMUM NUMBER OF ITERATIONS FOR SOLVER	300
MASS-LUMPING ON H	1
CONTINUITY CORRECTION	YES
MASS-LUMPING ON VELOCITY	0
SUPG OPTION	0;0;0;0
DISCRETIZATIONS IN SPACE	11;11
TYPE OF ADVECTION	1;5

A.2 Settings of TOMAWAC module

Table A-3: Wave model settings for Series A, B, C and D.

Parameter	**Setting**
NUMBER OF DIRECTIONS	36
MINIMAL FREQUENCY	0.05
NUMBER OF FREQUENCIES	24
TIME STEP	120
NUMBER OF ITERATIONS FOR SMALL SCALE PROCESSES	8
FREQUENTIAL RATIO	1.1
BOUNDARY DIRECTIONAL SPREAD 1	2
TYPE OF BOUNDARY DIRECTIONAL SPECTRUM	6
LIMIT SPECTRUM MODIFIED BY USER	YES
CONSIDERATION OF A WIND	YES
LINEAR WAVE GROWTH	1
WIND GENERATION	3
STATIONARY WIND	NO
MINIMUM WATER DEPTH	0.1
CONSIDERATION OF SOURCE TERMS	YES
TRIAD INTERACTIONS	0
WHITE CAPPING DISSIPATION	2
NON-LINEAR TRANSFERS BETWEEN FREQUENCIES	1
BOTTOM FRICTION DISSIPATION	1
SURFACE ROLLERS	YES
BETA S SURFACE ROLLERS	0.07
DEPTH-INDUCED BREAKING DISSIPATION	10
DEPTH-INDUCED BREAKING 1 (BJ) HM COMPUTATION METHOD	2
DEPTH-INDUCED BREAKING 1 (BJ) COEFFICIENT GAMMA2	0.7
DEPTH-INDUCED BREAKING 1 (BJ) COEFFICIENT GAMMA1	0.8
DEPTH-INDUCED BREAKING 1 (BJ) COEFFICIENT ALPHA	0.8
NUMBER OF ITERATIONS FOR THE SOURCE TERMS	1
NUMBER OF BREAKING TIME STEPS	4
NUMBER OF SURFACE ROLLER TIME STEPS	20
REMOTE STORAGE OF CHARACTERISTICS	YES

A.3 Settings of GAIA module

Table A-4: Sediment transport model settings for Series A.

Parameter	**Setting**
FINITE VOLUMES	NO
TYPE OF WAVES	1
BED LOAD FOR ALL SANDS	YES
SUSPENSION FOR ALL SANDS	NO
BED-LOAD TRANSPORT FORMULA FOR ALL SANDS	4
NUMBER OF LAYERS FOR INITIAL STRATIFICATION	1
CLASSES TYPE OF SEDIMENT	NCO;NCO
CLASSES SEDIMENT DENSITY	2650.;2650.
CLASSES SETTLING VELOCITIES	-9;-9
CLASSES SHIELDS PARAMETERS	-9;-9
CLASSES SEDIMENT DIAMETERS	0.0002;0.0005
LAYERS INITIAL THICKNESS	100.;0.
LAYERS NON COHESIVE BED POROSITY	0.4;0.4
SLOPE EFFECT	YES
FORMULA FOR SLOPE EFFECT	1
SEDIMENT SLIDE	YES
EFFECT OF WAVES	YES
BETA	1.6
FORMULA FOR DEVIATION	2
PARAMETER FOR DEVIATION	1.6

Table A-5: Sediment transport model settings for Series B.

Parameter	**Setting**
FINITE VOLUMES	NO
TYPE OF WAVES	1
BED LOAD FOR ALL SANDS	YES
SUSPENSION FOR ALL SANDS	NO
BED-LOAD TRANSPORT FORMULA FOR ALL SANDS	11
NUMBER OF LAYERS FOR INITIAL STRATIFICATION	1
CLASSES TYPE OF SEDIMENT	NCO;NCO;NCO;NCO;NCO; NCO;NCO;NCO;NCO;NCO
CLASSES SEDIMENT DENSITY	2650;2650;2650;2650;2650; 2650;2650;2650;2650;2650
CLASSES SETTLING VELOCITIES	-9;-9;-9;-9;-9;-9;-9;-9;-9;-9
CLASSES SHIELDS PARAMETERS	-9;-9;-9;-9;-9;-9;-9;-9;-9;-9
CLASSES SEDIMENT DIAMETERS	0.0001;0.0002;0.0003;0.0004;0.0005; 0.0006;0.0007;0.0008;0.0009;0.001
LAYERS INITIAL THICKNESS	100.;0.
LAYERS NON COHESIVE BED POROSITY	0.4;0.4;0.4;0.4;0.4;0.4;0.4;0.4;0.4;0.4
SLOPE EFFECT	YES
FORMULA FOR SLOPE EFFECT	1
SEDIMENT SLIDE	YES
EFFECT OF WAVES	YES
BETA	1.6
FORMULA FOR DEVIATION	2
PARAMETER FOR DEVIATION	1.6

Table A-6: Sediment transport model settings for Series C and D.

Parameter	**Setting**
FINITE VOLUMES	NO
TYPE OF WAVES	1
SCHEME FOR ADVECTION OF SUSPENDED SEDIMENTS	15;15;15;15;15;15;15;15;15;15
SCHEME OPTION FOR ADVECTION OF SUSPENDED SEDIMENTS	1;1;1;1;1;1;1;1;1;1
BED LOAD FOR ALL SANDS	NO
SUSPENSION FOR ALL SANDS	YES
BED-LOAD TRANSPORT FORMULA FOR ALL SANDS	11
SUSPENSION TRANSPORT FORMULA FOR ALL SANDS	5
SETTLING LAG	NO
EQUILIBRIUM INFLOW CONCENTRATION	YES
NUMBER OF LAYERS FOR INITIAL STRATIFICATION	1
CLASSES TYPE OF SEDIMENT	NCO;NCO;NCO;NCO;NCO; NCO;NCO;NCO;NCO;NCO
CLASSES SEDIMENT DENSITY	2650;2650;2650;2650;2650; 2650;2650;2650;2650;2650
CLASSES SETTLING VELOCITIES	-9;-9;-9;-9;-9;-9;-9;-9;-9;-9
CLASSES SHIELDS PARAMETERS	-9;-9;-9;-9;-9;-9;-9;-9;-9;-9
CLASSES SEDIMENT DIAMETERS	0.0001;0.0002;0.0003;0.0004;0.0005; 0.0006;0.0007;0.0008;0.0009;0.001
LAYERS INITIAL THICKNESS	100.;0.
LAYERS NON COHESIVE BED POROSITY	0.4;0.4;0.4;0.4;0.4;0.4;0.4;0.4;0.4;0.4
SLOPE EFFECT	YES
FORMULA FOR SLOPE EFFECT	1
SEDIMENT SLIDE	YES
EFFECT OF WAVES	YES
BETA	1.6
FORMULA FOR DEVIATION	2
PARAMETER FOR DEVIATION	1.6
WAVE INDUCED TURBULENCE	1
CROSS SHORE CURRENT	1
CROSS SHORE ASYMMETRY FACTOR	0.1
CROSS SHORE SKEWNESS FACTOR	0.3
CONSTANT NEAR BED CONCENTRATION RATIO	100
SEDIMENT SLIDE	YES
FRICTION ANGLE OF THE SEDIMENT	30

DEPARTMENT **MOBILITY & PUBLIC WORKS**
Flanders hydraulics

Berchemlei 115, 2140 Antwerp
T +32 (0)3 224 60 35
F +32 (0)3 224 60 36
flanders.hydraulics@vlaanderen.be
www.flandershydraulics.be